UNIVERSIDAD DE INVESTIGACIÓN DE TECNOLOGÍA EXPERIMENTAL YACHAY

Escuela de Ciencias Químicas e Ingeniería

TÍTULO: A CELLULOSE BASED COMPOSITE AS POTENTIAL ADSORBENT FOR THE REMOVAL OF HEAVY METAL IONS FROM WATER

Trabajo de integración curricular presentado como requisito para la obtención del título de Petroquímico

Autor:

Bastidas Peña Renny Jair

Tutores:

Ph.D Manuel Caetano Sousa

MSc. Lola De Lima Eljuri

Urcuquí, octubre 2021

Urcuquí, 11 de enero de 2022

SECRETARÍA GENERAL
(Vicerrectorado Académico/Cancillería)
ESCUELA DE CIENCIAS QUÍMICAS E INGENIERÍA
CARRERA DE PETROQUÍMICA
ACTA DE DEFENSA No. UITEY-CHE-2022-00003-AD

A los 11 días del mes de enero de 2022, a las 10:00 horas, de manera virtual mediante videoconferencia, y ante el Tribunal Calificador, integrado por los docentes:

Presidente Tribunal de Defensa	Dra. LOPEZ GONZALEZ, FLORALBA AGGENY , Ph.D.
Miembro No Tutor	Dra. HIDALGO BONILLA, SANDRA PATRICIA , Ph.D.
Tutor	Dr. CAETANO SOUSA MANUEL , Ph.D.

El(la) señor(ita) estudiante **BASTIDAS PEÑA, RENNY JAIR**, con cédula de identidad No. **1500855380**, de la **ESCUELA DE CIENCIAS QUÍMICAS E INGENIERÍA**, de la Carrera de **PETROQUÍMICA**, aprobada por el Consejo de Educación Superior (CES), mediante Resolución **RPC-SO-39-No.456-2014**, realiza a través de videoconferencia, la sustentación de su trabajo de titulación denominado: **A CELLULOSE BASED COMPOSITE AS POTENTIAL ADSORBENT FOR THE REMOVAL OF HEAVY METAL IONS FROM WATER.**, previa a la obtención del título de **PETROQUÍMICO/A**.

El citado trabajo de titulación, fue debidamente aprobado por el(los) docente(s):

Tutor	Dr. CAETANO SOUSA MANUEL , Ph.D.

Y recibió las observaciones de los otros miembros del Tribunal Calificador, las mismas que han sido incorporadas por el(la) estudiante.

Previamente cumplidos los requisitos legales y reglamentarios, el trabajo de titulación fue sustentado por el(la) estudiante y examinado por los miembros del Tribunal Calificador. Escuchada la sustentación del trabajo de titulación a través de videoconferencia, que integró la exposición de el(la) estudiante sobre el contenido de la misma y las preguntas formuladas por los miembros del Tribunal, se califica la sustentación del trabajo de titulación con las siguientes calificaciones:

Tipo	Docente	Calificación
Tutor	Dr. CAETANO SOUSA MANUEL , Ph.D.	9,0
Presidente Tribunal De Defensa	Dra. LOPEZ GONZALEZ, FLORALBA AGGENY , Ph.D.	9,5
Miembro Tribunal De Defensa	Dra. HIDALGO BONILLA, SANDRA PATRICIA , Ph.D.	10,0

Lo que da un promedio de: **9.5 (Nueve punto Cinco)**, sobre 10 (diez), equivalente a: **APROBADO**

Para constancia de lo actuado, firman los miembros del Tribunal Calificador, el/la estudiante y el/la secretario ad-hoc.

Certifico que *en cumplimiento del Decreto Ejecutivo 1017 de 16 de marzo de 2020, la defensa de trabajo de titulación (o examen de grado modalidad teórico práctica) se realizó vía virtual, por lo que las firmas de los miembros del Tribunal de Defensa de Grado, constan en forma digital.*

BASTIDAS PEÑA, RENNY JAIR
Estudiante

Firmado electrónicamente por:
RENNY JAIR BASTIDAS

FLORALBA AGGENY LOPEZ GONZALEZ
Digitally signed by FLORALBA AGGENY LOPEZ GONZALEZ
Date: 2022.01.17 13:27:22 -05'00'

Dra. LOPEZ GONZALEZ, FLORALBA AGGENY , Ph.D.
Presidente Tribunal de Defensa

Dr. CAETANO SOUSA MANUEL , Ph.D.
Tutor

Firmado electrónicamente por:
MANUEL CAETANO

SANDRA PATRICIA HIDALGO BONILLA
Firmado digitalmente por SANDRA PATRICIA HIDALGO BONILLA
Fecha: 2022.01.11 20:43:27 -05'00'

Dra. HIDALGO BONILLA, SANDRA PATRICIA , Ph.D.
Miembro No Tutor

Firmado electrónicamente por:
MARIELA SOLEDAD YEPEZ MERLO

YEPEZ MERLO, MARIELA SOLEDAD
Secretario Ad-hoc

AUTORÍA

Yo, **RENNY JAIR BASTIDAS PEÑA**, con cédula de identidad 1500855380, declaró que las ideas, juicios, valoraciones, interpretaciones, consultas bibliográficas, definiciones y conceptualizaciones expuestas en el presente trabajo; así cómo, los procedimientos y herramientas utilizadas en la investigación, son de absoluta responsabilidad de el/la autora (a) del trabajo de integración curricular. Así mismo, me acojo a los reglamentos internos de la Universidad de Investigación de Tecnología Experimental Yachay.

Urcuquí, octubre 2021.

Firmado electrónicamente por:
RENNY JAIR BASTIDAS

_____

Renny Jair Bastidas Peña

CI:1500855380

AUTORIZACIÓN DE PUBLICACIÓN

Yo, **RENNY JAIR BASTIDAS PEÑA**, con cédula de identidad 1500855380, cedo a la Universidad de Tecnología Experimental Yachay, los derechos de publicación de la presente obra, sin que deba haber un reconocimiento económico por este concepto. Declaro además que el texto del presente trabajo de titulación no podrá ser cedido a ninguna empresa editorial para su publicación u otros fines, sin contar previamente con la autorización escrita de la Universidad.

Asimismo, autorizo a la Universidad que realice la digitalización y publicación de este trabajo de integración curricular en el repositorio virtual, de conformidad a lo dispuesto en el Art. 144 de la Ley Orgánica de Educación Superior

Urcuquí, octubre 2021.

Firmado electrónicamente por:
RENNY JAIR BASTIDAS

Renny Jair Bastidas Peña

CI:1500855380

This page is intentionally left blank.

To my Father and Mother, Ángel and Miriam,

and my whole family.

Acknowledgments

First of all, I want to thank Yachay Tech University for allowing me to study at this high-level institution with international standards. Thanks to them, I met a world of researchers who guided me. Second, within this long path that has been my career as a bachelor, I thank the school of chemistry and engineering sciences for always being willing to help us with the laboratories and their excellent academic staff.

I also want to thank my tutors for this work. They were a fundamental pillar to be developed this thesis with the high standards that they are used to working with. They taught me that hard work has its reward and that when you are close to giving up, keep up the fight because at the end of the road, there will always be a great reward. To Professor Manuel and Professor Lola, thank you for your patience and time that you devoted to me in this present work, part of this work I owe entirely to them.

In addition, I want to make a particular emphasis on the entire faculty of the school of chemical sciences and engineering, who were my professors. Alicia Sommer who always had time for me and guided me with my academics. Thanks to Marvin Ricaurte and Alfredo Viloria, I understood what it is to work in an industry and the responsibilities that fall on new professionals in this branch. Juan Pablo Tafur taught me that honest and correct work could be achieved in public universities. Alex Palma taught me that a person could work in different areas, it is difficult to adapt, but it is not impossible. Hortensia Rodríguez taught me that mediocrity has no place in academia. I am infinitely grateful for the opportunity to share my knowledge in the sports field, and I leave a formative base for future students to make use of it, the table tennis club. Finally, to my friends who have accompanied me throughout this university career journey, I would not have been able to form the personal character that I achieved. A special dedication to Elizabeth Mariño and the School of Geology; School of Biology; Carlos Reinoso and the School of Physics for the use of their equipment.

Thank all those who make the Yachay Tech family the best in education in the Ecuadorian country.

Dedication

I dedicate this work to my family, who have been with me all the time. To my father, Ángel, who never lacked emotional and physical support when I needed it most, thank you for being a fundamental pillar not only to finish this university stage but in my entire life. To my mother, Miriam, for teaching me that actions define the human being and that you can always change and be a better person as long as you want it that way. Thanks, uncles and aunts. I hope to be an excellent example for my brothers. Finally, to the Tonato-Ñacato family, for making me a member of their family.

A special dedication to my grandfather Washington Bastidas who rests in peace. He taught me that if you are happy in life, you are already a millionaire. Thank you for dedicating your life and your emotions to me, Renny Bastidas.

Thank you, Grandparents; you are the most extraordinary beings in the family.

Thank you, Yachay Tech family, who are now part of me, I am leaving the institution, but I will always carry you in my heart.

RESUMEN

El propósito de este trabajo es obtener un hidrogel compuesto de carboximetilcelulosa (CMC), quitosano (CH), ácido cítrico (CA) y glicerol (GL), que se pueda usar para eliminar metales pesados en soluciones acuosas y ser utilizados como un método de tratamiento en aguas residuales. Este trabajo se enfoca en proponer materiales alternativos con aplicaciones interesantes a través del desarrollo de un hidrogel con la capacidad de adsorber especies de cerio (Ce). Se sabe que el cerio genera problemas ambientales que afectan a muchas personas en su salud. Los compuestos CMC / CH / AC / GL fueron clave para la formación del hidrogel, proporcionando a su estructura grupos carboxilo, hidroxilo y aminas. El glicerol desempeñó un papel esencial en la preparación de hidrogel, siendo el plastificante del mismo. El ácido cítrico fue el que promovió la reticulación química en la mezcla de componentes. Una vez que se verificó la función del hidrogel, los análisis químicos y morfológicos se llevaron a cabo a través de varias técnicas de caracterización, mediante el uso de espectroscopía infrarroja con transformada de Fourier (FTIR) y de foto emisión de rayos X (XPS). Además, se evaluó la capacidad de hinchamiento del gel de desorción, la espectroscopia de rayos X y la microscopía electrónica de barrido.

Además, mediante espectroscopía visible ultravioleta (UV-Vis) fue posible evaluar la funcionalidad del hidrogel para la remoción de iones de cerio en fase acuosa a través del análisis de los gráficos (tiempo vs. absorbancia). Una vez que los hidrogeles se liofilizaron, adquirieron un aspecto homogéneo y elástico. Algunos hidrogeles presentaron grados de plasticidad. La razón principal fue las diferentes cantidades de ácido cítrico (6, 12, 24 y 48 mL) se utilizaron para sintetizar el compuesto de hidrogel. En este caso, el ácido cítrico es el reticulante químico. Fue útil comparar grados de absorción entre diferentes compuestos de hidrogel. De la información obtenida por las técnicas de caracterización, se pudo evidenciar que el hidrogel formado presentó reticulación física y química. Sugiriendo que la unión de ácido cítrico con quitosano y carboximetilcelulosa produce cadenas, enlaces de amidas y grupos éster; ayudando a enriquecer las propiedades de absorción del hidrogel.

Palabras claves: Hidrogeles, Adsorbente, Reticulación, Composite, Medio Acuoso.

ABSTRACT

The purpose of this work is to obtain a hydrogel composed of carboxymethylcellulose (CMC), chitosan (CH), citric acid (CA), and glycerol (GL) which can be used to remove heavy metals from aqueous solutions and as well as in treatment methods in wastewater. This work focuses on proposing alternative materials with interesting applications by developing a hydrogel with the capacity to adsorb ion cerium species (Ce). Cerium is known to cause environmental problems that affect human health. CMC / CH / AC / GL compounds were the key to forming the hydrogel, providing its structure with carboxyl groups, hydroxyl, and amines. Glycerol played an essential role in the preparation of hydrogel, being the plasticizer of it. Citric acid was the one who promoted chemical reticulation cross-linking in the mixture of components. Once the hydrogel function was verified by being evaluated, chemical processes and morphological analyses using infrared spectroscopy with Fourier transform (FTIR) and X-ray photoemission (XPS). In addition, the swelling capacity of the desorption gel, X-ray electron photoemission spectroscopy, and scanning electron microscopy.

In addition, visible ultraviolet spectrophotometry (UV-Vis). The functionality of the hydrogel as cerium removal was verified through the analysis of graphs time vs. absorbance. Once the hydrogels were freeze-dried, having a homogeneous and elastic appearance. Some hydrogels presented degrees of plasticity. The main reason was that the different amounts of citric acid (6, 12, 24, and 48 mL) were used to synthesize the hydrogel compound. In this case, citric acid is the chemical reticulant. From the information obtained by the characterization techniques, hydrogel occurs through formed presented physical and chemical reticulation. It is suggested that the union of citric acid with chitosan and carboxymethylcellulose produces chains and bonds of amides also ester groups, helping to enrich the absorption properties of the hydrogel.

Key Words: Hydrogels, Adsorbent, Reticulation, Composite, Aqueous Medium.

Table of Contents

LIST OF TABLES

LIST OF FIGURES

CHAPTER I

1. INTRODUCTION

Hydrogel is understood as a three-dimensional network of flexible chains made up of elements connected in a certain way and swollen by a liquid. It is also known for its ability not to dissolve in water and to have a flexible and robust structure[1]. In addition, hydrogels contain hydrophilic functional groups attached to the polymeric skeleton that, because these groups, possess the ability to absorb water or a liquid of specific material. In contrast, the resistance to dissolution is due to cross-links between the network chains[1]. Some hydrogels have unique characteristics like adsorption or absorption capacity. Adsorption is a process in which an increase in the concentration of a particular component on the surface or interface between two phases exists. For the adsorption process to exist either on a liquid or solid surface, the atoms on the surface are subject to unbalanced attraction forces normal to the surface plane, which are responsible for the adsorption phenomenon[2]. Adsorption has been a fundamental piece for the treatment of wastewater[3]; focusing on the removal of contaminants from the water. Due to the adsorption process which is simple, efficient, economical, and friendly with the environment, it is considered to be one of the best for sustainable development in the future[4]. For the next generation, it is very important to conserve natural reservoirs all clean without pollutants like heavy metals. For this reason, hydrogels research has a big area for treatment water.

Water is the central resource that humans need for their survival, thus it is necessary to take care of this non-renewable supply[5]. Water pollution is a global issue caused by most of the humans who do not correctly use water and continue to pollute uncontrollably[6]. According to the United Nations[7], more than 80% of the world's wastewater does not have adequate treatment or an environmentally friendly discharge. It is therefore essential to conserve existing freshwater reserves and to seek to improve wastewater treatment techniques. As far as wastewater is concerned, there are solid compounds and other substances that are different from clean water; one of them is heavy metals.

Heavy metals can be found in the environment and therefore can enter the body of humans and animals. There is a misconception that heavy metals are bad for human health. The truth is that a small amount of these metals (depends on the metal) is essential for the metabolism of humans and animals. When metals exceed the amounts allowed in the body, it can lead to severe health problems due to their toxicity[8].

The metal subjected to adsorption tests in this study is cerium; this metal has been booming in recent years because its use has been maximized in industrial applications of nanoparticles. Therefore, there is a minimal record of deaths and diseases in humans or aquatic and terrestrial organisms. Cerium was used as a drug in the early 1900s. It has also been involved in the automobile industry, used as an additive to improve gasoline or its derivatives[9]. This metal can seriously damage lungs depending on size metal causing a disease called pulmonary embolism. Inhalation or direct ingestion are the main ways to get the disease. For this reason, in recent years, efforts have doubled to find treatments that can remove the metal cerium from the environment[8,9]. In addition, it is known that coagulants, flocculants, and disinfectants are used in water treatment plants, such as materials that help remove this type of heavy metals[9]. One of these treatments is use of hydrogels, which is economical, simple and friendly with the environment. In the present work, CMC and CH are the main components of the hydrogel.

There are several studies in which CMC and CH compounds have been involved. According to Lifeng Yang[10], these two substances CMC and CH are zwitterionic species, that is, function as anions and cations. Therefore, the union of them is given by their affinity and provides new properties to the resultant material. Super adsorbent was formed because these unions.

1.1 PROBLEM APPROACH

The global environmental problem has different external causes, and one of them is due to accumulation of heavy metals. A heavy metal refers to any high-density metallic chemical element that is toxic at even low concentrations and affects human health[11]. Industrialization is the main reason why pollution increase over time. Industries contaminated oceans and rivers with heavy

metals, toxic wastes, and others effluents due to the release of waste disposal into the environment[12]. Environmental pollution can be very harmful to people's health because if a human consumes it, it can lead to poisoning and catastrophic diseases such as cancer. In addition, animals living in aqueous environments are also adversely affected by the problem of heavy metals, as they suffer consequences such as premature death or poor deformations in their genetic structure[13,14].

There are several technologies for the removal of metal content in aqueous media. These are membrane filtration, chemical precipitation, adsorption[15,16], ion exchange, electrolytic methods, reverse osmosis, and solvent extraction[16]. Of all these methods, adsorption is considered one of the most suitable for eliminating heavy metals in aqueous media. Moreover the use of the adsorbent based on biomass obtained from simulating cellulose is a sustainable and cost-effective idea since it has a low impact on the food chain of people and the low impact of hydrogel production.[17–19]

The use of the cellulose derivatives, like CMC, with chitosan will be tested for the development of hydrogels. Subsequently, it can be used on a large scale as these products or substances are found in great quantity worldwide. Specifically, in Ecuador, it can be found in oversized proportions and even in the residues of shrimp shells[20]. Thanks to this research work, the quality of people's standard of living will improve and help to reduce the environmental pollution currently taking place by the industries that pollute the freshwater tributaries.

1.2 OBJECTIVES

1.2.1 GENERAL OBJECTIVE

The general objective of this study is to synthesize and characterize a hydrogel based on chitosan, carboxymethylcellulose, citric acid, and glycerol and evaluate its potential as adsorbent for removal of ion Ce (IV) from aqueous solutions.

1.2.2 SPECIFIC OBJECTIVES

- To prepare hydrogels based on composites CMC and CH by sustainable methodologies
- To determine the structure and surface chemistry of the synthesized compound by X-Ray Diffraction (XRD) and X-Ray Photoelectron Spectroscopy (XPS).
- To evaluate morphological properties of hydrogel by Scanning Electron Microscopy
- To verify the functional groups of the hydrogels by Attenuated Total Reflectance-Fourier Transform Infrared Spectroscopy (ATR-FTIR).
- To perform a study of adsorption for the metal ion cerium (IV) in order to provide information about the kinetics of the process the mass transfer mechanisms.
- To analyze the desorption of hydrogels and its swelling capacity in different pH media.
- To determine the best-qualified hydrogel composition for adsorption process for cerium ions removal.

CHAPTER II

2. BACKGROUND AND LITERATURE REVIEW

2.1 Hydrogels

Conventional hydrogels have limited mechanical strength and do not resist temperature changes[21]. According to current research, new hydrogels are more resistant due to the cross-linking which refers to a bond or a short sequence of bonds that links one polymer chain to another. There are two types of cross-linking in hydrogels: chemical and physical. Chemical cross-linking works in a permanent configuration due to covalent bonds used as an esterifying agent and high temperatures[22]. On the other hand, in physical cross-linking, there is a non-permanent configuration due to the interaction by hydrogen bonds, ionic forces, hydrophobic forces, and natural reticulation between the different fibrils of the polymer[21–23].

The characteristics of an excellent hydrogel are high capacity of absorption in saline solution; the lowest amount of solution and monomer used in this preparation, low price, high durability and stability under standard conditions during storage. Furthermore, an efficient hydrogel adsorbent is the one that can be recycled. It should not produce organic or synthetic waste in order to help to combat environmental pollution.

2.1.1 Classification of hydrogels

In recent years, synthetic hydrogels have replaced natural hydrogels. The reason is that synthetic hydrogels have unique characteristics that natural hydrogels lack[1]. These characteristics are long life of the hydrogel, high absorption capacity, and a larger vital mechanical force. These characteristics are attributed to the cross-linking that exist to produce synthetic hydrogels.

The different several types of hydrogels can be classified according it origin, as indicated in Table 1[1].

Table 1. Types of hydrogels based on origin.

According to:	
Its source	Natural or of Synthetic origin
Its polymeric composition	• Homopolymeric • Copolymeric • Multipolymer
Its configuration	-
Its physic structure and chemical composition	• Amorphous (non-crystalline) • Semicrystalline: A complex mixture of amorphous and crystalline phases • Crystalline.
Their cross-linking	Degree of cross-linking
Their physical appearance	• Matrix • Film • Microsphere
The electrical charge of the network	• Non-ionic (neutral) • Ionic (including anionic or cationic) • Amphoteric electrolyte (ampholytic) containing both acidic and basic groups • Zwitterionic (polybetaines) containing both anionic and cationic groups in each structural repeating unit.

Taken from Ahmed[1]

From the following techniques[1] gels can be synthetized. The necessary steps are always involving monomer, initiator, and cross-linker species

2.1.2 Preparation of hydrogels

The scientific advance in the preparation of hydrogels has expanded the way to make a hydrogel by adding more polymers and copolymers synthesized by inverse suspension, emulsion polymerization, and solution polymerization[1].

One of them, and the most important for the new technologies for the preparations of the hydrogels, is bulk polymerization. It consists of many monomers and can be formed with one or more types of monomers. In Figure 1 the primary process for this technology is shown.

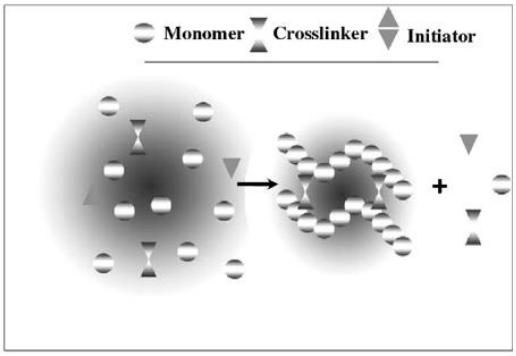

Figure 1. Schematic diagram showing the process of hydrogel preparation[1] by bulk polymerization.

Other new techniques have been divided into solution polymerization/cross-linking, suspension polymerization or inverse-suspension polymerization, grafting to support, polymerization by irradiation[1].

To follow the ideal process for reproducing a hydrogel, varying the monomers or concentrations that make the hydrogel unique is shown an illustrative diagram in Figure 2.

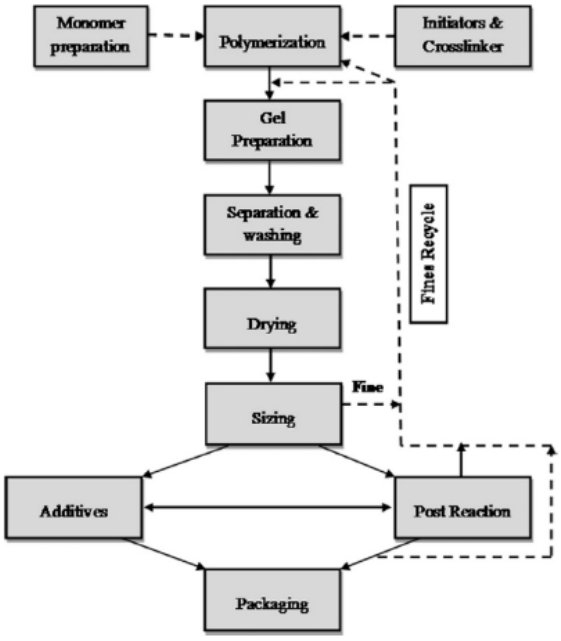

Figure 2. Hydrogel preparation block diagram (solution polymerization/cross-linking procedure)[1]

Over the years some attempts have been made to produce better hydrogels than previous ones, and the production of so-called superabsorbent polymer (SAPs), has been achieve mainly used in agriculture. It has also been possible to obtain super porous hydrogels (SPHs). They are categorized as a highly adsorbent polymer system. Based on these two super adsorbents, new technologies have been developed to assist in researching and improving the types of hydrogels[1,24].

Hydrogels with different shapes can be prepared, such as cubic, hollow tube, rod, sheet, and film. The discovery of new combinations of materials, generating suitable composites, has helped to improve the mechanical properties, thermal, optical, electrical, among others features of hydrogels[25].

Table 2. Various types of chemical and physical hydrogels.

Cross link	**Methods**	**Polymers**	**Applications**
Physically cross-linked or self-assembled hydrogel	Freeze-thawing	Polyvinyl alcohol (PVA)/Chitosan, PVA/Starch, PVA/PVA/Gelatin, PLGA.	Therapeutic applications, Tissue engineering[26,27]
	Stereo complex formation	Dextran, Poly (lactic acid), Poly (ethylene glycol).	Drug delivery, Biomedical and pharmaceutical[2,28,29]
	Ionic interaction	Cellulose microfilms, Alginate.	Drug delivery, Antigen delivery[3]
	H-Bonding	Chitosan, Hyaluronic acid Theragnostic.	Drug delivery, Cyclodextrin, biomedical, Cartilage tissue[4,30]
	Maturation (heat-induced aggregation)	Cyclodextrin, polypseudorotaxane Alginate capsules.	Soft tissue engineering, cell scaffold, regenerative medicine and cartilage repair[31]
Chemically cross-linked hydrogel	Chemical cross-linking hydrogel	Whey protein Poly (ethylene glycol), TGP, Collagen.	Biomedical, Agriculture and horticultural, Tissue engineering, water purification, drug delivery[32,33]

Grafting	Chitosan-cellulose Poly(Ɛ-caprolactone), poly(ethylene glycol), Carboxymethyl cellulose, styrene, sulfonate.	Antibacterial, antifouling[34]
Radical Polymerization	N-Viniylcaprolactam, Chitosan Poly (ethylene glycol) methyl ether Methacrylate.	Controlled delivery[35,36]
Condensation reaction	Beta-Cyclodextrin, Cellulose nanofiber.	Advanced Bio catalysis and tissue engineering, wound dressing, packing biomaterial[28,37].
Enzymatic reaction	Poly (ethylene glycol), Methacrylate, chitosan.	Biomedical Application
High energy reaction	Poly (oligo (propylene glycol) Methacrylate), Poly (vinyl methyl ether).	

Taken from Sharma and Tiwari[38]

2.1.3 Hydrogel applications

Generally, hydrogels are divided into categories showed in Table 1, and depending on the category its application. The most common uses of hydrogels are: hygienic products, agriculture, drug delivery systems, sealing, coal dewatering, artificial snow, food additives, pharmaceuticals, biomedical applications tissue engineering and regenerative medicines, diagnostics, wound dressing, separation of biomolecules or cells[15] and barrier materials to regulate biological adhesions, and Biosensor[24]. Their use as in agricultural water absorbents in combination with biopolymers by grafting hydrophilic monomers onto starch and other polysaccharides[1,24].

The main characteristic of the new hydrogels is the reinforcement of their structure and unions, resulting in a swelling capacity much higher than that of previous generations of hydrogels[25].

2.2 Adsorption

The term adsorption refers to the accumulation of molecules in the interfacial layer, while the term desorption carries out the release of such molecules[28].In addition, adsorption will depend on the surface area of the adsorbent and the material used in the experiment. For this reason, all industrial adsorbents have surface areas[28,29].

Below, in Table 3, some key definitions related to adsorption and desorption processes are presented.

Table 3. Definitions: Adsorption.

Term	**Definition**
Adsorption	Enrichment of one or more components in the vicinity of an interface
Adsorbate	Substance in the adsorbed state
Adsorptive	Adsorbable substance in the fluid phase
Adsorbent	Solid material on which adsorption occurs
Chemisorption	Adsorption involving chemical bonding
Physisorption	Adsorption without chemical bonding

Taken from Rouquerol [29].

In the description of the adsorption, important to divide it into physical and chemical adsorption. Physisorption involves relatively weak inter-modular forces and is fully reversible. In addition, it allows the desorption of the evaluated experienced material under standard conditions. In contrast, chemisorption involves the formation of a chemical bond between the sorbate molecule and the

surface of the adsorbent[33]. In addition, during the chemisorption, the evaluated material undergoes an irreversible change and loses its original form[34].

After knowing which kind of adsorption and how adsorption works, the following is to know the kinetic models to calculate adsorption at a specific time. Due to the parameters of the models, it is possible to optimize the pathways of the adsorption mechanism, expresses the dependence of the surface properties of the adsorbent with the results of adsorption, in addition to determining adsorbent capacities and effectively designing adsorption systems[32,39]. Kinetics allows us to establish the appropriate times when the hydrogel must be submerged in the liquid medium for its absorption.

Once the parameters for kinetic adsorption models have been established, the following is to perform adsorption isotherms, which will help us learn more about the speed at which adsorption occurs and the mathematical expression that must be expressed. The adsorption isotherm is the first source of information in an adsorption process, formerly also referred to as excess adsorption by scientist Gibbs more than 100 years ago[35], scientists like Wagner, Verschaffeldt, Guggenheim, and others suggest a quantitative and qualitative analysis for each of the experiments performed.

2.2.1 Adsorption Isotherms

Several types of adsorption isotherms provide qualitative information about the adsorption process and the degree of surface coverage by the adsorbate. According to Emmet and Teller[36], isotherms are classified into five primary forms, shown in Figure 3. Type I isotherms are associated with systems in which adsorption does not advance beyond the mono-molecular layer. The other types of isotherms involve the formation of multiple layers.

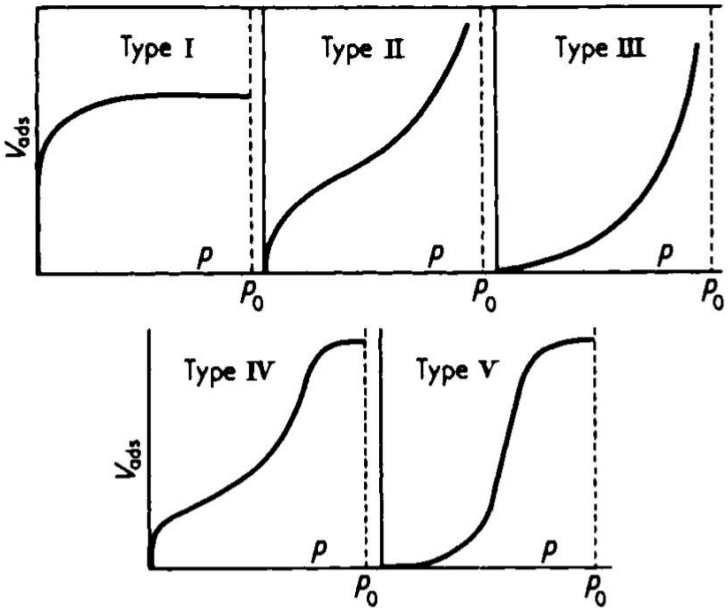

Figure 3. The five typical shapes of isotherms for physical adsorption. Reproduced from Brunauer et al.[36]*,courtesy of American Chemical Society.*

The science of adsorption helps to find equations that fit much more closely to the actual state of the material. According to the recommendation of the IUPAC[40], the micropores have a width that does not exceed 2 nm, the mesopores have a width between 2 and 50 nm, while the macropores have a width greater than 50 nm[40,41].

2.2.1.1 Adsorption kinetics models

Adsorption kinetic models are used to evaluate the performance of the adsorbent and to examine mechanisms of adsorption. The process of mass transfer during adsorption have been summarized in three steps[42].

1) External diffusion. The adsorbate diffuses through the thin liquid film around the adsorbent, driving by the difference in chemical potential between the adsorbate in the bulk solution and the adsorbate at the surface of the adsorbent.
2) Internal diffusion. The adsorbate diffuses in the pores of the adsorbent.
3) Adsorption of the adsorbate in the active sites of the adsorbent.

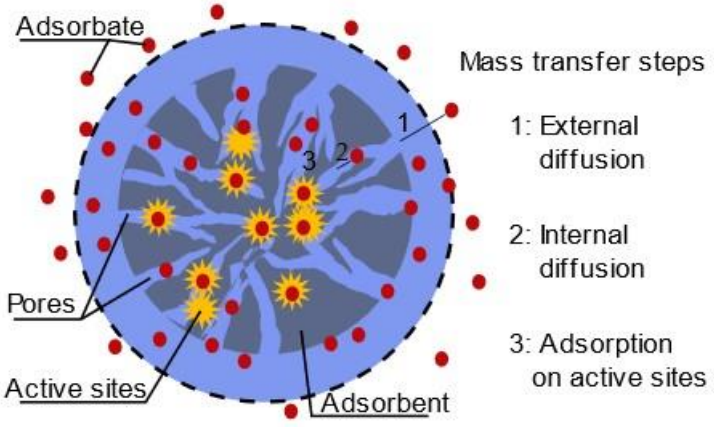

Figure 4. Adsorption mass transfer steps[42].

2.2.1.1.1 Kinetics models

Different adsorption reaction models have been used to investigate the adsorption kinetic process. These models include: (1) empirical models (without specifical physical meaning), (2) external diffusion models, which assume that the slowest step in the process is the diffusion of adsorbate from the bulk solution and through a boundary liquid film around the adsorbent, (3) internal diffusion models, which assume that the diffusion of adsorbate within adsorbent is the slowest step, (4) adsorption onto active sites models, which assume that the adsorption onto active site is the slowest step[42].

The most applied models are empirical (pseudo-first-order and pseudo-second-order). However, the lack of specific physical meanings makes it impossible to establish the mass transfer mechanisms using these empirical kinetic models unless some physical meaning has been established. On the other hand, models of phenomenological external/internal and adsorption inactive sites require complicated solving methods.

The linear regression method is the most widely used to fit data and obtain the parameters of adsorption models, thanks to its simplicity. However, the linearization process could introduce propagating errors to the independent/dependent variables, causing inaccuracy in the estimation of the parameters[43,44].That is why it is advisable to use a nonlinear method, to obtain consistent and accurate estimations for model parameters[43,44]. In the next equation, to obtain (Q), is calculated by the difference between the initial (C_o) and the instantaneous metal concentration (C) for knowing the amount of metal adsorbed at time (t):

$$Q(mg.g^{-1}) = \frac{C_o - C}{D} \quad (1).$$

$Q_{max}(mg.g^{-1})$ is the maximum amount of metal adsorbed by the adsorbate.

D is a constant surface of metal

Crank model

Crank's model[45] describes a homogeneous diffusion of an adsorbate into an adsorbent modeled as a sphere and assuming a constant surface diffusivity D_s at all points of the particle is:

$$\frac{\partial Q}{\partial t} = \frac{D_s}{r^2}\frac{\partial}{\partial r}\left(r^2\frac{\partial Q}{\partial r}\right) \quad (2), r\ being\ the\ distance\ in\ the\ radial\ direction.$$

This equation works perfectly for the average concentration in the solid at a given time for the case when the sphere is initially free of solute, and the solute concentration on the surface remains constant (there must be no external mass transfer). From the central Crank equations are derived two, which play different roles in both time and absorbance. For short times, or more precisely for $Q/Q_{max} < 0.3$, there is a simplified equation, and for longer times, that is $Q/Q_{max} > 0.85$, there is another equation known as Boyd[46]. The equations will be presented in the equation summary in Table 15.

Weber and Morris

Weber and Morris[47] who proposed this adsorption model experimented on batches of activated carbon alkylbenzenes. Two equations were presented, which are:

$$\frac{Q}{Q_{max}} = Cte \times \ t^{1/2} \quad (3)$$

$$\frac{Q}{Q_{max}} = Cte \times \ t^{1/2} + Cte' \quad (4)$$

Equation (3) and (4). The big difference between these two equations is Cte', which explains the external mass transfer that is not negligible. Although many researchers have discussed this last equation, assuming there is no reason why the amount of metal adsorbed on $t = 0$ is different from zero.

Bangham model

It is understood as the generalization of the Weber and Morris model or applying the Freundlich model[48] to kinetics, so taking into account the chemical nature of the surface. See equation in Table 15.

Complex diffusional model

The pore surface and volume diffusion model (PVSDM) were suggested by Geankoplis and Leyva-Ramos[49]. PVSDM is an example of a complex model as its use focuses on the mathematical part, and the more parameters there are, the more difficult it will be to find a congruent solution. See equation in Table 15.

2.2.1.1.2 Adsorption models

Adsorption is considered the slowest process, that usually happens when the process is chemical or irreversible. To understand the following equations presented below, S are the adsorption sites, M is the adsorbate, C is the concentration of the adsorbate in solution, γ the order of reaction to the adsorbate, SM is the concentration of adsorbate bound to the sorbent, k_{ad} is the constant adsorption of velocity and k_d is the constant of desorption velocity. The sorption rate is equal to dQ/dt.

Different kinetic models were considered to describe the data. In Table *15*, the differential and integrated form of the equations for each model is showed.

Pseudo-first order model

This model[50] presented is by the non-reversible equation:

$$S + M \rightarrow MS \quad (5)$$

In addition, it is based on five assumptions, which are:

1. Sorption occurs only at localized sites, and there is no interaction between sorbed ions.

2. Adsorption energy does not depend on surface coverage

3. The maximum adsorption corresponds to a monolayer saturated with adsorbates on the adsorbent surface.

4. The concentration of M is considered constant.

5. The absorption of metal ions in activated coals is governed by a first-order speed equation.

To detail the empirical formula, we have that the sorption rate is:

$$k_{ad}C^{\gamma}\left(\frac{Q_{max}-Q}{Q_{max}}\right)^{1} = K'_{ad}(Q_{max}-Q) \quad (6),$$

The integral equation and non-linear form can be found in Table 15.

Pseudo second-order model

The kinetics[39] of metal ion removal has the following equation:

$$2S + M \rightarrow M(S)_2 \quad (7)$$

The assumptions as the first-order model are the same, except that a second-order speed equation governs the absorption of metal ions in activated coals due to affinity. Thus, the sorption speed can be written as:

$$k_{ad}C^{\gamma}\left(\frac{Q_{max}-Q}{Q_{max}}\right)^{2} = K'_{ad}(Q_{max}-Q)^{2} \qquad (8)$$

The integral equation and non-linear form can be found in Table 15.

Pseudo n order for n different from zero

The kinetics[51] of metal ion removal for a pseudo-n-order model is presented as follows:

$$nS + M \rightarrow M(S)_n \quad (9)$$

This model's characteristics are the same as the first order, except for second-order, since a speed of order n governs the absorption of metal ions in activated coals. Therefore, the equation would be written in this way:

$$k_{ad}C^{\gamma}\left(\frac{Q_{max}-Q}{Q_{max}}\right)^{n} = K'_{ad}(Q_{max}-Q)^{n} \quad (10)$$

The integral equation and non-linear form can be found in Table 15.

Langmuir model

For the kinetics of metal ion removal using the Langmuir[52] model using this reversible equation:

$$S + M \rightleftarrows MS \quad (11)$$

It uses the same principles for the first-order model, but the desorption rate is not negligible compared to the adsorption rate. Thus, the sorption rate can be written as:

$$k_{ad}C^{\gamma}\left(\frac{Q_{max}-Q}{Q_{max}}\right) - k_d\left(\frac{Q}{Q_{max}}\right) = K'_{ad}(Q_{max}-Q) - K_dQ \quad (12)$$

The integral equation and non-linear form can be found in Table 15.

Elovich model

The kinetics of the removal of metal ions for Elovich[52] model, is presented as follows:

$$S + M \rightarrow MS \quad (5)$$

Unlike the first-order model, this postulate has the following characteristics:

1. Sorption occurs only at localized sites, and there is no interaction in sorbate ions.

2. The bonding energy increases linearly as the surface is covered, according to the law:

$$Ea = Ea_0 + RT\beta Q \quad (13)$$

Then, the adsorption rate constant k_{ad} can be written, using the Arrhenius equation, as:

$$k_{ad} = Cte \times \exp\left(-\frac{Ea}{RT}\right) = \propto' \times \exp(-\beta Q) \quad (14)$$

$$\text{with } \propto' = Cte \times \exp\left(-\frac{Ea_0}{RT}\right) \quad (15)$$

3. The concentration of M is considered constant

4. The absorption of metal ions in activated coals is negligible before the exponential (i.e., by a zero-order velocity equation). Therefore, the sorption speed can be written as:

$$\propto \times \exp(-\beta Q) \quad (16)$$

$$\text{with } \propto = C^{\gamma} \propto' \quad (17)$$

The integral equation and non-linear form can be found in Table 15.

Freundlich model

This postulate is widely used for aqueous systems and is expressed as[53]:

$$\frac{x}{m} = K{C_e}^{1/n} \quad (18)$$

Where x = the amount of solute adsorbed, m = the weight of adsorbent, C_e = the solute equilibrium concentration, K and $1/n$ = constants characteristics of the system.

The Freundlich equation is an empirical equation that encompasses the heterogeneity of the surface and the exponential distribution of sites and their energies[54,55]. When it wants to linearize the Freundlich equation, it is written it logarithmically as:

$$log\frac{x}{m} = logK + \frac{1}{n}logCe \quad (19)$$

BET model

Brunauer developed the BET[52] isotherm, Emmet and Teller said work consists of generalizing the ideal localized monolayer treatment (Langmuir model), taking into account the multilayer adsorption[36]. According to the postulate, each molecule in the first adsorbed layer serves as a site for the adsorption of a molecule into the second and so on. The expression of the isotherm BET comes from a kinetic argument presented for the Langmuir isotherm or a thermodynamic argument since it works correctly for both[33,54]. The resulting equation for the BET equilibrium isotherm is:

$$V = \frac{V_m BP}{(P_o - P)[1 + (B-1)P/P_o]} \quad (20)$$

Where V and V_m have the same meaning as in the Langmuir isotherm, P_o = saturation vapor pressure of the saturated liquid sorbate, and B = a constant:

$$B = \frac{a_1 a_2}{a_2 a_1} e^{(E_I - E_L)/RT} \quad (21)$$

Which can be simplified to:

$$B = e^{(E_I - E_L)/RT} \quad (22)$$

Where a_1 and a_2 = rates of condensation on the first and second layers, b_1 and b_2 = rates of evaporation from the first and second layers, E_I = first layer heat adsorption, and E_L = heat of liquefication pf the bulk phase.

The term $E_I - E_L$ is known as the net heat of adsorption. Thus, the BET equation provides a measure of both the heat of adsorption and the surface area of the solid. Application of the BET equation to the adsorption from solution takes the from:

$$X = \frac{X_m B C}{(C_s - C_e)[1 + (B-1)C_e/C_s]} \quad (23)$$

Where X, X_m, and C_e have the same meaning as in Langmuir's isotherm, and C_s = solubility of the solute in water at a specified temperature. Transforming Equation 1.53 to:

$$\frac{C_e}{X(C_s - C_e)} = \frac{1}{X_m B} + \frac{(B-1)}{X_m B}\frac{C_e}{C_s} \quad (24)$$

shows that a plot of the left side against C_e/C_s should give a straight-line having slope $(B-1)/X_m B$ and intercept $1/X_m B$.

Henry's Law: Linear Adsorption model

Henry's[52] law is the simple postulate in which the amount adsorbed varies directly with the equilibrium concentration of the solute. It is known as Henry's law by the analogous isotherm for the solution of gases in liquids. Represented in the following equation:

$$X = K_h C_e \quad (25)$$

where $X = x/m$, the amount of solute adsorbed by unit mass of adsorbent; C_e = equilibrium concentration; and K_h = a constant.

This isotherm is used for low solute concentrations. The linear ratio is usually observed at the lowest concentration levels of a total adsorption isotherm. Almost all adsorption isotherms are

reduced to Henry's law at low concentrations. Yielding bC_e is small compared to the unit, so the equation is reduced to:

$$X = X_m bC_e \quad (26)$$

Attributed to Henry's Law.

2.2.2 Proposal Adsorption

The majority of adsorption studies have been carried out in distilled water as the primary solution in the experimentation. In addition, inorganic salts have been shown to affect the adsorption capacity of specific components such as activated carbon in selected solutes[56,57]. Therefore, it is necessary to carry out further studies to support this approach and help propose adsorption systems that do not affect the proper functioning of adsorbents in different media other than distilled water.

2.3 Wastewater approach

Wastewater often contains toxic pollutants from anthropogenic industries, such as mining or agricultural plants lacking environmentally friendly techniques, or natural forces such as volcanoes, earthquakes, or storms[58]. These pollutants are classified into three main groups: organic, inorganic and biological particles[58,59]. The main problem is that most Latin American countries do not have protocols or techniques to help reduce this type of environmental pollution[58,59].

Table 4. Typical characteristics of untreated wastewater.

Component	**Concentration Range**
Biochemical oxygen demand (BOD_5)	100 – 360 mg/L
Chemical oxygen demand	250 – 100 mg/L
Total organic carbon (TOC)	80 – 300 mg/L
Total Kjeldahl nitrogen (TKN)	20 – 85 mg/L as N

Total phosphorus	5 – 15 mg/L as P
Oil and grease	5 – 120 mg/L
Total solids (TS)	400 – 1200 mg/L
Total dissolved solids (TDS)	250 – 850 mg/L
Total suspended solids (TSS)	110 – 400 mg/L
Volatile suspended solids (VSS)	90 – 320 mg/L
Fixed suspended solids (FSS)	20 – 80 mg/L
Settleable solids	5 – 20 mL/L
Total coliforms (TC)	106 – 1010 MPN/100mL
Fecal coliforms (FC)	103 – 108 MPN/100mL

Taken from Riffat[60],USA.

2.3.1 Wastewater treatment

It can find bacteria, protozoa, worms, viruses, fungus in the polluted waters, among others. The presence of these infectious organisms causes severe diseases in the human body, such as typhoid fever, dysentery, cholera, jaundice, hepatitis, among others[5,61]. It is also found heavy metals, which is where the problem of this work lies, as research is being carried out to eradicate this problem of heavy metals in aqueous environments and polluted waters. Water treatment is done by dictating specific ways of disinfecting polluted water, which can also be considered techniques or technological procedures to help clean up polluted water[62]. Now, to remedy these kinds of problems, a disinfectant must be able to destroy all kinds of pathogens like bacteria and organic waste, must function within the ambient temperature range, must be safe and easy to handle, should provide residual protection against decontamination, among others.

Table 5. Conventional methods associated with primary, secondary and tertiary wastewater treatments.

Primary Treatment	**Secondary Treatment**	**Tertiary Treatment**
Sedimentation	Activated Sludge	Filtration
Flotation	Aeration	Adsorption
Screening	Biological Filters	Chlorination
Neutralization	Anaerobic Treatments	Ozonation
Homogenization		Ionic Exchange
		Micro-sieving
		Reverse Osmosis

Taken from Ramalho[63] et al.

The main problem focuses on the presence of metals in the water solution, for this reason a table has been made in which the levels allowed worldwide are considered, according to National Secondary Drinking Water Regulations (NSD).

Table 6. Summary of NSD Water Regulations.

Contaminant	**Secondary Standard**
Aluminum	0.05 to 0.2 mg/L
Chloride	250 mg/L
Color	15 (color units)
Copper	1.0 mg/L
Corrosivity	Noncorrosive
Fluoride	2.0 mg/L

Foaming Agents	0.5 mg/L
Iron	0.3 mg/L
Manganese	0.05 mg/L
Odor	3 threshold odor number
pH	6.5 – 8.5
Silver	0.10 mg/L
Sulfate	250 mg/L
Total Dissolved Solids	500 mg/L
Zinc	5 mg/L

Taken from Riffat[60].

2.3.2 Wastewater in Ecuador

In Ecuador, the increase in artisanal and illegal mining has led to increased pollution by heavy metals in the province of El Oro, which causes severe damages in areas near rivers or effluents. We speak specifically of the province of El Oro because history tells us that this city has been exploited in the mining aspect over the years, and the repercussions currently having are the waters polluted mainly in the rivers[64]. In the Ecuadorian Amazon, the minerals riverside have also been exploited, causing strong environmental pollutants in freshwater tributaries. The concentrations of heavy metals in the soils, the product of the cyanidation. Moreover, the amalgamation tailings have levels that exceed the limits established according to Ecuadorian regulations[65].

In 2007, the National Mining Company "ENAMI" was established with the idea of using a change in the energy matrix. The creation of this company was to make Ecuador a large-scale mining country[66]. There are still clandestine companies that do not comply with the disposition of the Ecuadorian state and continue to pollute the waters with heavy metals.

Mining companies have acted without social responsibility and have neglected the safety and health of people exposed to these pollutants[64,66]. It is essential to take this situation very seriously because residents or people close to these places can contract serious diseases such as cancer or improper development of growth in the next generations.

The industrial sector in Ecuador is constantly growing, and therefore, it is essential to foresee the use of water today and in the future. The wastewater that comes from Ecuadorian industries is mostly treated by the company ENAMI. However, there is no protocol for small and medium-sized companies that usually exist most in Ecuador and cause a large percentage of environmental pollution in the waters[67].

Municipalities of Ecuador have carried out an investigation percentage about regulations for drinking water. The following data was obtained of the municipalities 90% comply with the regulations for drinking water treatment; 2% buy treated water, and 8% have no treatment. In Tena has not been found the exact data on the amount of water treatment plant volume. However, it is possible to verify that the majority of Amazonian provinces comply with the regulatory standards[58,68]. Thus, 80% of Amazonian provinces, including the province of Napo, comply with the INEN 1108 standard.

Although Ecuador has several water sources, it is essential to carry out a protocol, which helps record the use and waste caused by each municipality in the country[69]. In the Ecuadorian Andean region, what most affects the waters of the rivers or waters of the subsoil is agriculture; water consumption is very excessive. Going to accurate percentages in Ecuador, it is distributed as follows how it is divided; agricultural sector (81%), households (13%), and industry (6%)[67],according to (Directory of Companies and Establishments DIEE-2013)[67]. The importance of the industry for the management of water resources in Ecuador stems not only from the level of water consumption but, more importantly, from the pollution that results from their production processes[70].

The lack of adequate regulation to improve environmental controls puts the Ecuadorian country in trouble since, as mentioned above, the industries will grow in the future. There will be a more significant water demand, and therefore, there will be more wastewater.

Wastewater must be taken very seriously in all the municipalities of Ecuador. Programs such as water treatment plants and awareness of the use of water for citizens should already be addressed in the meetings of the burgomasters of each city in the country of Ecuador.

One of the possible solutions for implementing this type of protocol in the Ecuadorian country would be to increase the price of water, as this would allow more money to be invested in sustainable and environmentally friendly projects[71]. It is emphasized, this is a possible solution because this work does not focus on the economic aspect, and there is no technical study that validates what it is about complementing as a possible solution, for a better type of water in Ecuador and as a type of water regeneration.

2.4 About heavy metals

The term heavy metals refer to any metal element or metalloid that has a 3 $g.cm-3$ relatively high density ranging from 3.5 to 7 $g.cm-3$ and is toxic or poisonous at low concentrations and includes mercury (Hg), cadmium (Cd), arsenic (As), chromium (Cr), thallium (Tl), zinc (Zn), nickel (Ni), copper (Cu) and lead (Pb), among others[8].

A summary in Table 7 has been made to show the damage that heavy metals can cause to the human body.

Table 7. The standard metal concentration in drinking water and the health effects.

Metal	**Effects**	**Drinking Water Standards**
Lead	• Toxic to humans, fauna and livestock	By the Environmental Protection Agency maximum concentration: 0.1mg L^{-1}
	• High doses cause metabolic poison	By European Community: 0.5 mg L^{-1}

	• Tiredness, irratibility, anemia and behavorial changes of children • Hipertension and brain damage • Phytotoxic	Regulation of water quality (India) 0.1 mg L^{-1}
Nickel	• High conc. cause DNA damage	By the Environmental Protection Agency maximum concentration: 0.1mg L^{-1}
	• Eczema of hands	By European Community: 0.1 mg L^{-1}
	• High phytotoxicity	Regulation of water quality (India) 0.1 mg L^{-1}
	• Damaging Fauna	
Chromium	• Necrosis nephritis and death in man (10mg kg-1 of body weight as hexavalent chromium)	By the Environmental Protection Agency maximum concentration: (hexavalent and trivalent) total 0.1mg L^{-1}
	• Irritation of gastrointestinal mucosa	By European Community: 0.1 mg L^{-1} Regulation of water quality (India) 0.1 mg L^{-1}
Copper	• Causes damage in a variety of aquatic fauna	By the Environmental Protection Agency maximum concentration: 0.1mg L^{-1}

	• Phytotoxic	By European Community: 3 mg L^{-1}
	• Mucosal Irritation and corrosion	Regulation of water quality (India) 0.01 mg L^{-1}
	• Central nervous system irritation followed by depression	
Zinc	• Phytotoxic	By the Environmental Protection Agency maximum concentration: 5mg L^{-1}
	• Anemia	By European Community: 5 mg L^{-1}
	• Lack of muscular coordination	Regulation of water quality (India) 0.01 mg L^{-1}
	• Abdominal pain etc.	
Cadmium	• Cause serious damage to kidneys and bones in humans	By the Environmental Protection Agency maximum concentration: 0.005mg L^{-1}
	• Bronchitys, emphysema, anemia	By European Community: 0.2 mg L^{-1}
	• Acute effects in children	Regulation of water quality (India) 0.001 mg L^{-1}
Mercury	• Poisonous	By the Environmental Protection Agency maximum concentration: 0.002mg L^{-1}

	• Causes mutagenic effects	By European Community: 0.001 mg L^{-1}
	• Disturbs the cholesterol	Regulation of water quality (India) 0.004 mg L^{-1}
Arsenic	• Causes toxicological and carcinogecnic effects	World Health organization guideline of 10 $\mu g\ L^{-1}$
	• Causes melanosis, keratosis and hyperpigmentation in humans	By European Community: 0.01 mg L^{-1}
	• Genotoxicity trough, generation of reactive oxygen species and lipid peroxidation	Regulation of water quality (India) 0.05 mg L^{-1}
	• Immunotoxic	
	• Modulation of Co recepetor expression	

Taken from Sanjay K. Sharma[8]

2.4.1 Cerium approach

Cerium is a member of the rare metal lanthanide family. It is the most abundant and, after europium, the most reactive rare earth metal as summarized by EPA 2009[72]. Cerium oxide (CeO_2) is commonly used as a catalyst in combustion reactions and is being used as an additive in diesel fuels; Cerium metal is also widely used in the pharmaceutical industry and agricultural products[72]. Cerium is a metal highly required in the metallurgy industry; also used as polishing agents for glass, plate glass, technology tubes, and lenses[73]. Previously, some of the heavy metals were essential for specific reactions carried out or essential for the metabolism of animals or people.

When the Cerium is used in any of these applications, it does not have a proper discharge to the wastewater treatment plants, so they go directly to nature and end up contaminating the environment in which they are[8,72].

The way Cerium enters the human body is through inhalation; as it is known, the compounds or derivatives of petroleum are, or most are very volatile. Cerium is quickly released from the reaction when it comes into contact with oxygen. Cerium, have reported adverse effects in the lungs, resulting in pneumoconiosis (unique effect of cerium metal) and severe lung problems[73]. Cerium is then associated with most lung problems in the industry; bronchitis, pneumonitis, and granulomatous lesions after sub-acute exposures are considered. European multi-center case study has reported an association between increased cerium concentrations and an increased risk of first myocardial infarction[73]. Also, Cerium oxide was detected in the liver and skeleton (but not in the spleen and kidneys)[73].

2.5 Characterization techniques

2.5.1 Attenuated Total Reflection – Fourier Transform Infrared Spectroscopy (ATR-FTIR)

The ATR-FTIR equipment is defined as Fourier transform infrared spectroscopy with attenuated total reflectance. This robust method reveals the details of chemical reactions in the solid solution interface[74,75]. In addition, spectroscopy research offers the possibility of a more direct understanding of how organic ligands adsorb on mineral surfaces[76].

The principle of this technique is based on the absorption of infrared radiation by molecules that produce the bonds' vibration. The vibratory range in the infrared is described between wavelengths from 2.5 to 25μm[76]. This absorption process of infrared radiation is known as a quantified process; the molecules only absorb a small amount of energy. The change recorded in the IR spectrum is in the order of 8-40 KJ/mol[76].

These types of equipment will find two types of operation; Disperse and Fourier Transform (FT-IR) instruments. The two types of instrumentation are used for different cases. It should be emphasized that the ATR-FTIR technique is the one that was used in this work and is the most used today for speed efficiency and produces faster data. See in Figure 5. below for a representation of the IR spectrophotometer.

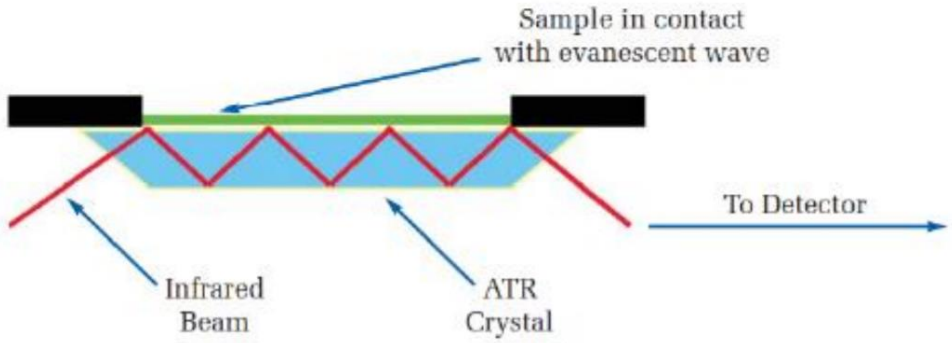

Figure 5. Simple scheme ATR-FTIR measurement in plane[76].

2.5.2 X-Ray Diffraction (XRD)

According to A.W. Hull[77], the operation of XRD equipment has its pattern independently of the other substances, regardless of the material from which it is made. Each sample tested on the XRD has its fingerprint; therefore, the dust diffraction method is ideal for the characterization and identification of polycrystalline phases[78]. Understanding XRD. The X-rays emanating from the machine are in a wavelength range of 0.5 -2.5°A; for these rays to occur, the elements in the sample must be sufficiently charged with kinetic energy[78]. In addition, you have to be very careful with the noise in the diffraction program produced by some transition metals because this gives some erroneous data. The operation of the powder X-ray diffractor is based on the reflection geometry between the X-ray source and the detector. Based on the Bragg-Bertano diffractometer[79], the

sample is irradiated with the help, and then the refractive beam is focused on the detector. See in Figure 6.

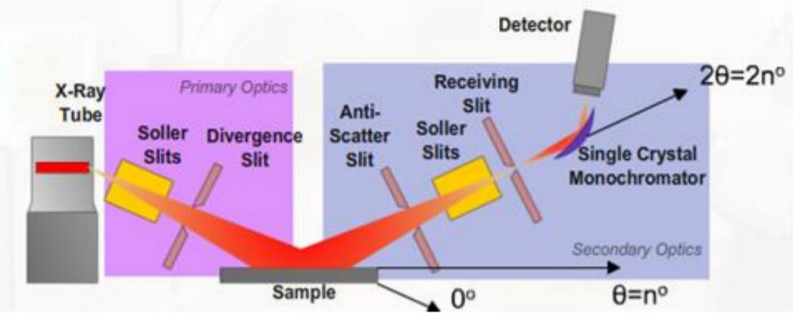

Figure 6. Scheme of the Braggs-Bentano diffractometer[78]

2.5.3 X-Ray Photoelectron Spectroscopy (XPS)

XPS, a powerful technique used to learn how metal ions bind to matrices. In addition, XPS equipment has been used to characterize the structure of metal compounds and their interactions with membranes and films made up of polymers, as well as their interactions with catalysts[80], algal biomass, yeast, and synthetic sorbents. Dambies et al[81]. used XPS equipment to characterize functional groups in specific adsorption mechanisms such as chitosan, depending on finding the possible mechanism of reduction after adsorption. Another essential feature of XPS operation is identifying the sorption sites involved in the accumulation of adsorbed species. Keep in mind; the samples should be dried at room temperature a day before[82].

2.5.4 Adsorption and desorption tests

2.5.4.1 Ultraviolet – Visible (UV-Vis) Spectrophotometry. (Adsorption evaluation)

Spectrophotometric methods are more economical and more straightforward than methods such as chromatography and electrophoresis[83]. The UV-Vis technique is a helpful technique for extracting

qualitative and quantitative information from bands of analytes by interpreting results that can be used for the absorption of materials according to the light strip that reflects in the equipment.

The spectrophotometer produces a light signal (analog signal) and an electrical signal (digital signal). In addition, this equipment has a photomultiplier tube, photodiodes, and a diode array (diode array). See in Figure 7. for a diagram of the operation of the UV-VIS.

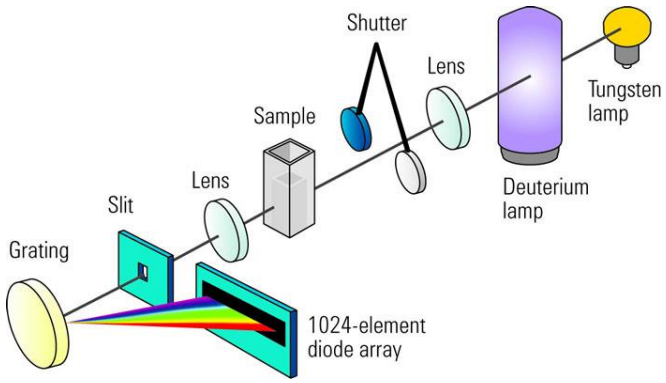

Figure 7. Scheme of an experimental arrangement in a UV-Vis with diode array equipment[84].

This type of equipment is used in the agricultural, pharmaceutical, and biomedical sectors, among others[83,85]. These equipment photodiode arrays are more sensitive than former equipment, high speed, have a low noise level, are more compact, and the cost is lower and easier to use[85,86].

It should ensure that the cells are quartz since when working with plastic and glass cells, the noise of the material affects the absorbance of the sample.

Also, it should ensure that the cell is clean and that there are no bubbles on the walls. Another widespread error is to use two different cell types for the target and the sample, so it is recommended to use the same cell as this way; the error will be much more minimal.

2.5.4.2 Desorption Test

The experiment was done to reuse or give a second life to the hydrogel that was already used. Once the hydrogel is with heavy metal molecules in the aqueous medium, the hydrogel was put back into an aqueous medium to desorb the metal and again be used to absorb another type of metal or the same metal that it had already absorbed.

According to Pietrelli, L.[48] et al., the efficiency of desorption agents be calculated by the difference in the weight of the hydrogel before absorption (X_{ma}) and the weight of the hydrogel after desorption (X_{md}), resulting in the following equation.

$$D_e\ (\%) = (X_{ma} - X_{md}) \times 100 \quad (27)$$

2.5.5 Morphological Study

The equipment is used to obtain 3D images of any solid sample. Stereomicroscopes have two main designs: Common Primary Objective (CMO) and Greenough, see in Figure 8.

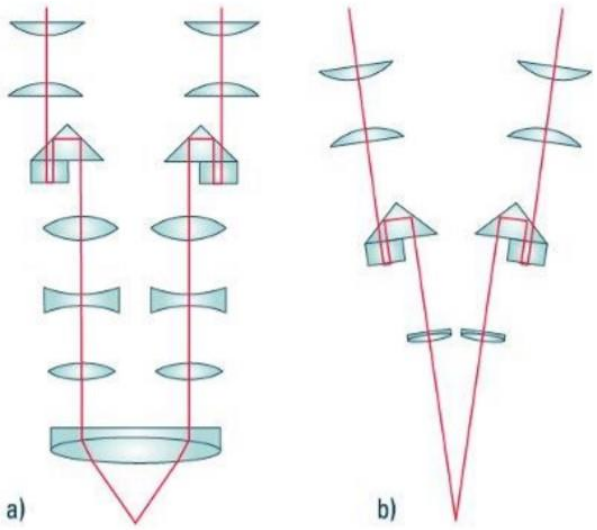

Figure 8. The two main stereomicroscope optical designs: (a) CMO. (b) Greenough[87].

Greenough is used in industry while CMO is used in research for their high resolution. The equipment to be used in the present investigation is the CMO, this focuses on the refraction of light by means of a single objective lens of great diameter through which the right and left ocular channels visualize the sample[87].

2.5.6 Swelling Study

The swelling test is part of the characterization of the absorption phase; this test was performed to verify the behavior of the hydrogels in the different media that are acid, neutral, and basic. The use of solutions media is to detail the best medium in which hydrogels can perform their function.

The following formula will therefore be used:

$$E_{sr}(\%) = \left(\frac{(W_s - W_d)}{W_d}\right) \times 100\% \quad (28)$$

where E_{sr} is the swelling ratio, W_d is the weight of the swollen hydrogel at time t and W_s is the weight of the dry hydrogel

Another reason for this test is that different hydrogels were performed with specific percentages of citric acid, leaving more accessible spaces for the water molecules to use those sites to see the change made by the highly specific hydrogel and analyze the absorbance capacity of each chemically modified hydrogel[88].

2.6 Components of hydrogel

2.6.1 Citric acid

Citric acid, also known as (2-hydroxy-1,2,3-propane tricarboxylic acid, C6H8O7), is a metabolite found in plants and animals. Pure citric acid is colorless, easily soluble in water, and has characteristics such as biodegradability, ecological, and molecule capture. Commercially, it is mainly found in soft drinks and effervescent salts that, together with CO_2, form a perfect combination. In hydrogels, citric acid helps form the amide groups and contributes to the adsorption or sequestration of certain materials in such research[89].

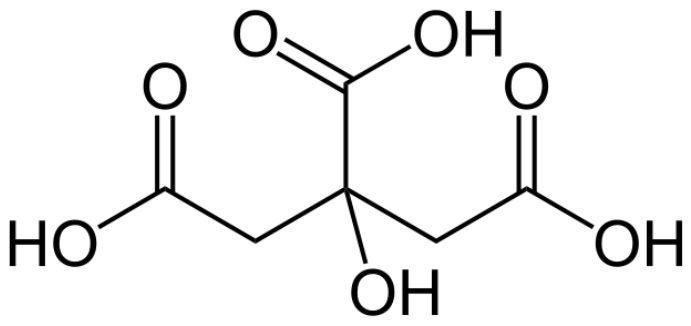

Figure 9. Structure of Citric Acid

Citric acid as Cross-linker has been successful from most tests with other materials, including protein fiber synthesis and up to biomedical applications. It has also been used as a cross-linking agent for biodegradable films due to its acidity. In addition, new composite materials are made as a plasticizer in hydrogels of a new generation[90]. Goyanes[91] and co-workers simply cross-linked

citric acid with starch using glycerol as a plasticizer by heating a mixture of starch, glycerol. The cross-linking between citric acid and glycerol has resulted in a notable improvement in the thermal and mechanical properties of the formed films. Thanks to these new techniques, the compound formed has also shown an excellent capacity for the duration in water or air, resulting in the function of citric acid, a preservative.

In addition to the properties as a new compound material that possesses citric acid, it has also been used as an excellent disinfectant combating viruses very dangerous to human tissues, for example, norovirus[90]. One of the uses that have been known for years is the removal of metal waste to clean the machinery of the industries[91].

2.6.2 Glycerol

Glycerol (1,2,3-propanetriol or glycerin) is an organic molecule. Glycerol has been produced from epichlorohydrin obtained from propylene (i.e., fossil petroleum). Its plasticizing power has increased its use in many new investigations, such as hydrogels or gelling of products in which cellulose is involved[92].

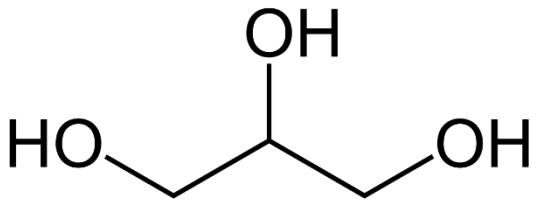

Figure 10. Structure of Glycerol

Glycerol, used in the pharmaceutical, cosmetic, and food industries[93]. Glycerol is an exciting product because it can be found naturally and in the petrochemical industry. Some of the characteristics of glycerol are: it is not toxic to humans either to nature depending to the quantity of glycerol, it is hygroscopic, and is clear and odorless[93]. Glycerol is entirely soluble in water and alcohol. However, it is insoluble in hydrocarbon. By using glycerol, the component provides more moisture to the composite materials increasing the viscosity of the formed solution[93]. Glycerol is very stable and can be stored at room temperature, in addition to having long duration[93].

2.6.3 Chitosan

Chitosan (a cationic polysaccharide composed of (1,4)-linked 2-amino-2-deoxy-β-D-glucan) is produced commercially, with the process of exhaustive deacetylation of chitin (> 60%). Chitin is a structural element in the exoskeleton of crustaceans or insects and is the second most abundant natural biopolymer after cellulose[94,95]. The sources of chitin are generally crabs and shrimp due to the abundance of these animals. In Ecuador, data were recorded in 2019 that explain its power in shrimp exports, thus reaching about 1,400 pounds per shrimp. Furthermore, this is not to mention the added value that this animal has in industry food[20,94].

This polymer known as chitosan differs from other polysaccharides by the presence of nitrogen in its molecular structure, its cationicity, and its ability to form polyelectrolyte complexes; It should be noted that it is soluble in water after the formation of carboxylate, formate, acetate, lactate, malate, citrate, glyoxylate, pyruvate, glycolate and ascorbate salts[95,96]. An important characteristic of chitosan is that it is biodegradable due to its low toxicity. For this reason, this material is involved in several areas, such as medicine and technology, since chitosan itself can be used as a combination for the formation of other compounds. Its physical-chemical characteristics help to improve thermodynamic conditions and mechanics of the new material generated[94,95].

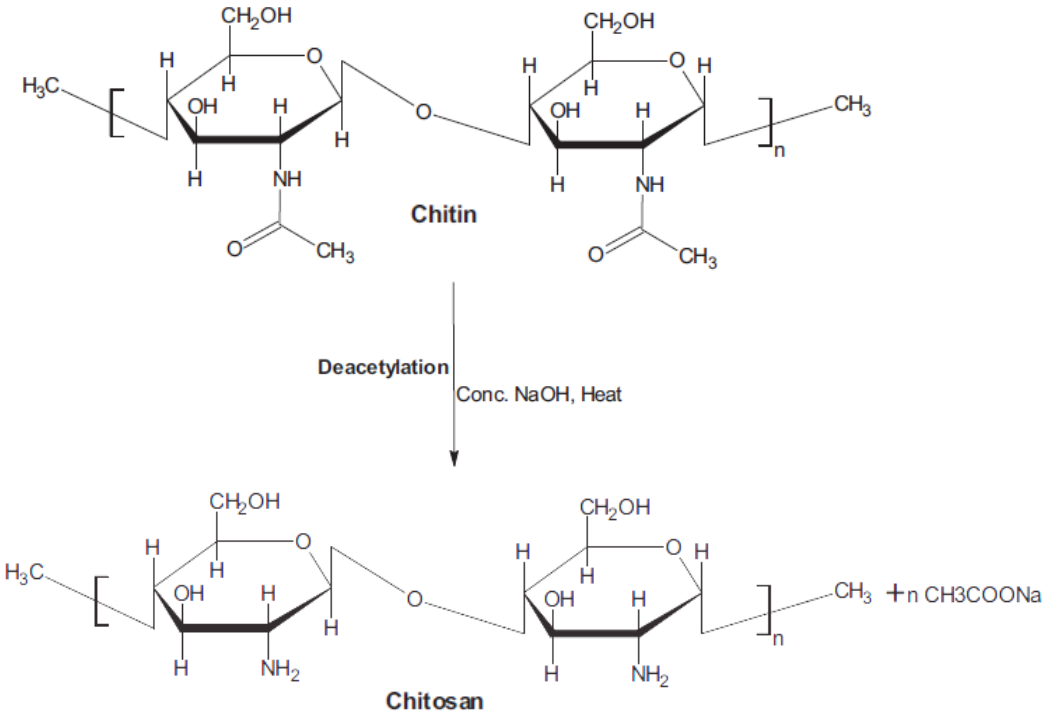

Figure 11. Deacitlyation of chitn to chitosan. Taken from S.K. Shukla et al./ International Journal of Biological Macromolecules

Chitosan has been related to the formation of gels and hydrogels due to its ability to mold the final product, making it possible to convert it into tablets, capsules, microparticles, sponges, among others[97].

To obtain the raw material chitosan, the Ecuadorian Pacific Ocean, also it is a great distributor of shrimp worldwide. Therefore, it is viable to create a chitosan factory in Ecuador. The only factory that has registration is located in Colombia. In addition, there will be an excellent benefit for the environment since the waste caused by these industries will not remain untreated; instead, they will be given a second in which it can be used to generate more jobs for Ecuadorians.

The shrimp industry in Ecuador is enormous, along with the flowers market and the banana market is established that is where gross money is most generated for the Ecuadorian country. Ecuador produces around 600 tons of shrimp in 2017[98].

According to the study carried out by Berrezueta[98]et al., 72 thousand tons of shrimp shells are available each year, allowing the weekly, monthly and annual supply of the creation of chitosan to export internationally, and there is no debasement. It was done to avoid the disruption of the human food chain, so only waste generated by shrimp industries was taken into account, which will be enough for the first processing plant in the country, Ecuadorians.

2.6.4 Carboxy methyl cellulose

Cellulose is one of the most abundant substances on the earth. So, this is a polymeric raw material with a versatile structure and unique properties that make them fascinating. Cellulose has its derivatives are methylcellulose, hydroxypropyl methylcellulose, carboxymethylcellulose, ethyl cellulose.

As mentioned above, Carboxymethylcellulose (carmellose) is a derivative of cellulose; being one of the most researched derivatives of cellulose. Thanks to its solubility in water; this solubility will depend on the degree of polymerization, the degree of substitution, and uniformity of the substitution distribution. This product can be found anywhere in the world, thanks to the ease of its training properties[99]. Carboxymethylcellulose is highly hygroscopic and quickly hydrates. Its commercial use is pervasive, but the main ones are drinks because of their viscosity to the final product. CMC has incredible characteristics such as hydrophilicity, biocompatibility, nontoxicity, pH-sensitivity, and gel-forming properties[100].

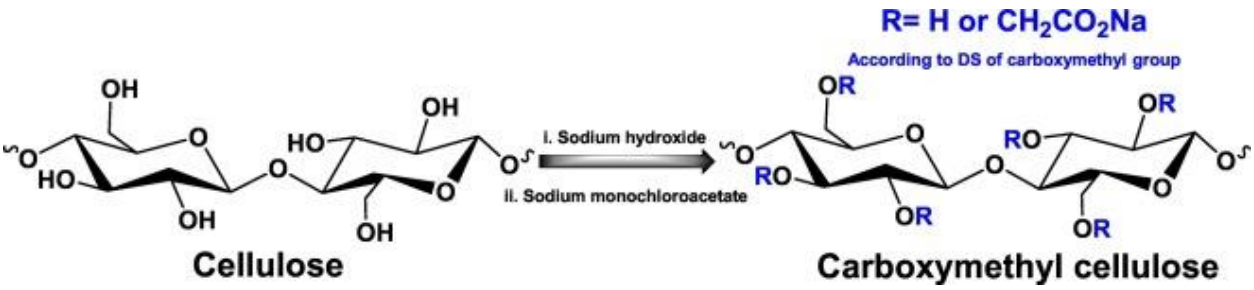

Figure 12. Synthesis and chemical structure CMC[100]

One of the unique properties that have earned him space in the food industry and medicine is that the CMC is very flexible, reaching to surpass some petroleum-based plastics and being an excellent absorbent[101].

2.7 New composite prepared

When a composite is formed, a synergistic effect is developed. The components' properties interact, causing an effect more significant than the sum of the effects they would cause separately[101]. The different materials of the composite work together to give the unique composite properties, resulting in an integrated performance. for a result of the new hydrogel.

Most of these materials were used because today, they can be found in oversized proportions and would not affect the food chain of people or animals. Therefore, these materials, besides being very beneficial for creating the hydrogel as a superabsorbent, also helps us against subtracting the effect of environmental pollution, thanks to the chemical components used with immense quantity and frequently used in the world of chemistry. The main reason, already described, should also be emphasized that these elements CMC/CH were taken into account because of their low cost, compared to obtaining graphene or commercial carbon molecules.

CHAPTER III

3. Methodology

3.1. Materials and Reagents

Table 8. Materials

Material	Description
Analytical Balance	Balance Cobos precision HR-150A
heating and stirring plate	Brand: TOPO; Model: MS 300H; Temp: 380°C; RPM: 1500; Voltage: 110V,60Hz
Ultrasound	Brand: Selecta Ultrasons H-D 3000865; Series: 613561; Capacity: 6L; Frequency: 40KHz; Power: 180W; Max. Temp: 80°C; Heating Power: 150W; Power Source: AC 220V/240V, 50/60 Hz
Stove	Brand: POL-EKO-APARATURA SP.J; Model: SLW 115 STD// Voltage: 230V-60Hz; Max. Temp: 300°C
freezer	Brand: Electrolux; Model: ERT44K6CMG; Series: 63602934
lyophilizer	Brand: LABCONCO; Serial: 191084517 I; Catalog No: 7670520
Spectrophotometer	Brand: analytik jena SPECORD S600 Diode array spectrophotometer; Power Source: 220V,149V
Mechanical press	Brand: Carver HYDRAULIC UNIT MODEL #3912; Model: 4386; S/N: 190380; Max. Ram Stroke: 5 1/8"

Table 9. Reagents.

Reagent	Description	Molecular Formule
Chitosan food grade (BioFitnest)	Food supplement, Purity: 100%	beta (1-4)-2-amino-2-desoxy-D-glucose
Acetic Acid glacial anhydrous for analysis	CAS-No: 64-19-7; Density: 1.05kg/l, Purity: 100%	CH COOH
Carboxymethyl cellulose sodium salt high viscosity	CAS-No: 9004-32-4; Viscosity 2% in water, 20 ºC, 1100-1900 cps; Extra Pure, Loba Chemie, sodium glycolate Max 0.4%	RnOCH2-COOH
Glycerol	CAS-No: 56-81-5, Purity: 99%; Molecular biology, Sigma Aldrich	C3H8O3
Citric Acid anhydrous	CAS-No: 77-92-9, Purity: 99.5%; Loba Chemie	C H O
Cerium Ethylenediaminetetraacetic (EDTA)	CAS-No: 6381-92-6; Purity: 99-101%	C10H16N2O8
Sulphuric Acid	CAS-No: 7664-93-9, Purity: 95-97% density: 1.84kg.	H2SO4

3.2. Synthesis of hydrogel

The present work synthesized hydrogels based on CH and CMC by a specific method known as solution polymerization/cross-linking. The method reported by Calderón[102] et al. was modified in this new research, adding one more lyophilizer step.

The experimental procedure was divided into four stages, which were carried out in the present work. In this way, it was possible to have an order of time and a sequence, since each stage worked depended on the previous one.

3.2.1 First Stage: Preparation of solutions.

In the first stage, solutions were prepared CH, CMC, CA, GL. Chitosan was taken to 2% (w / v) dissolved 2 g de CH in 2% (v / v) acetic acid. The solution formed by CH and AA reached a pH

of 6. Then, 2 g CMC was dissolved in 100 mL distilled water to obtain a solution 2% CMC (w / v). 2 g CA and10 mL GL were dissolved in 100 mL distilled water to obtain a solution of 2% (w / v) and 10% (v / v), respectively.

In all cases of solutions, approximately 3 hours were mixing required. Stirring was stopped when the compounds had crossed the molecules and were completely homogeneous. In Table 10, see the preparation of these solutions with their respective preparation details.

Table 10. Preparation of solutions for hydrogel synthesis.

Reagent	**Concentration**	**cantidad**	**Volumen (mL)**	**Solutions**
Chitosan	2% (w/v)	2 g	100mL solution 2% (v/v) AA	C1
CMC	2%(w/v)	2 g	100mL H20	C2
Citric Acid	2%(w/v)	2 g	100mL H20	C3
Glycerol	10%(v/v)	10 mL	90mL H20	C4

In addition, the reagents were weighted with an accuracy of 0.0001g in the analytical balance. See the visual form about all process corresponding to first stage in Figure 13.

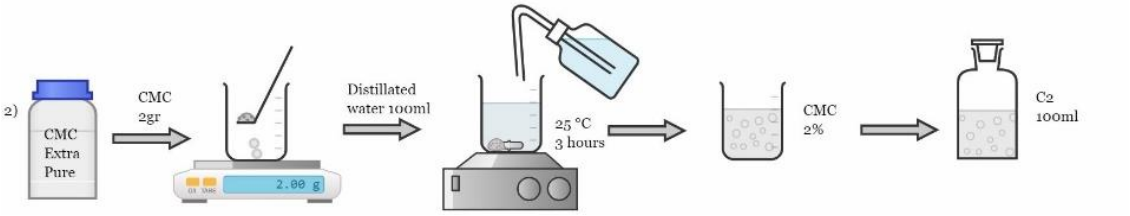

Figure 13. Scheme of processes performed in the first stage of synthesis (One of them; example to the new solution C2 by CMC dissolution.)

3.2.2 Second Stage: Preparation of Composite Hydrogels

The quantities used for the preparation of the hydrogels for each solution obtained in the first stage are presented in the Table *11*. The volume ratio of CH:CMC:GL was 3:1 remained constants and only varying concentrations of CA.

Table 11. Quantities used for the preparation of the hydrogel.

Hydrogel Samples	**6 CA**	**12 CA**	**24 CA**	**48 CA**
Reagent	**Trial 1**	**Trial 2**	**Trial 3**	**Trial 4**
CMC	24 mL	24 mL	24 mL	24 mL
CH	8 mL	8 mL	8 mL	8 mL
CA	6 mL	12 mL	24 mL	48 mL
GL	9 mL	9 mL	9 mL	9 mL

In Figure 14, see the scheme of the hydrogel's preparation process divided in 6 steps:

1) A commercial mixer was used to mix all solutions in an approximate time of 10 or 12 min. The order of the solution mixture was as follows: CMC, CH, CA, GL.

2) Hydrogels were drifting in centrifuge tubes to use an ultrasound bath for 40min at 40°C.

3) The stove was used to finish drying the hydrogel samples; during 40min at 80°C.

4) Hydrogel samples were carried to use a freezing at - 80°C.

5) Last step was to use the lyophilizer with the condition of -45°C and a pressure of 42 kPa.

6) Hydrogels are ready to use in different techniques characterization. All hydrogels' samples were labeled and stored.

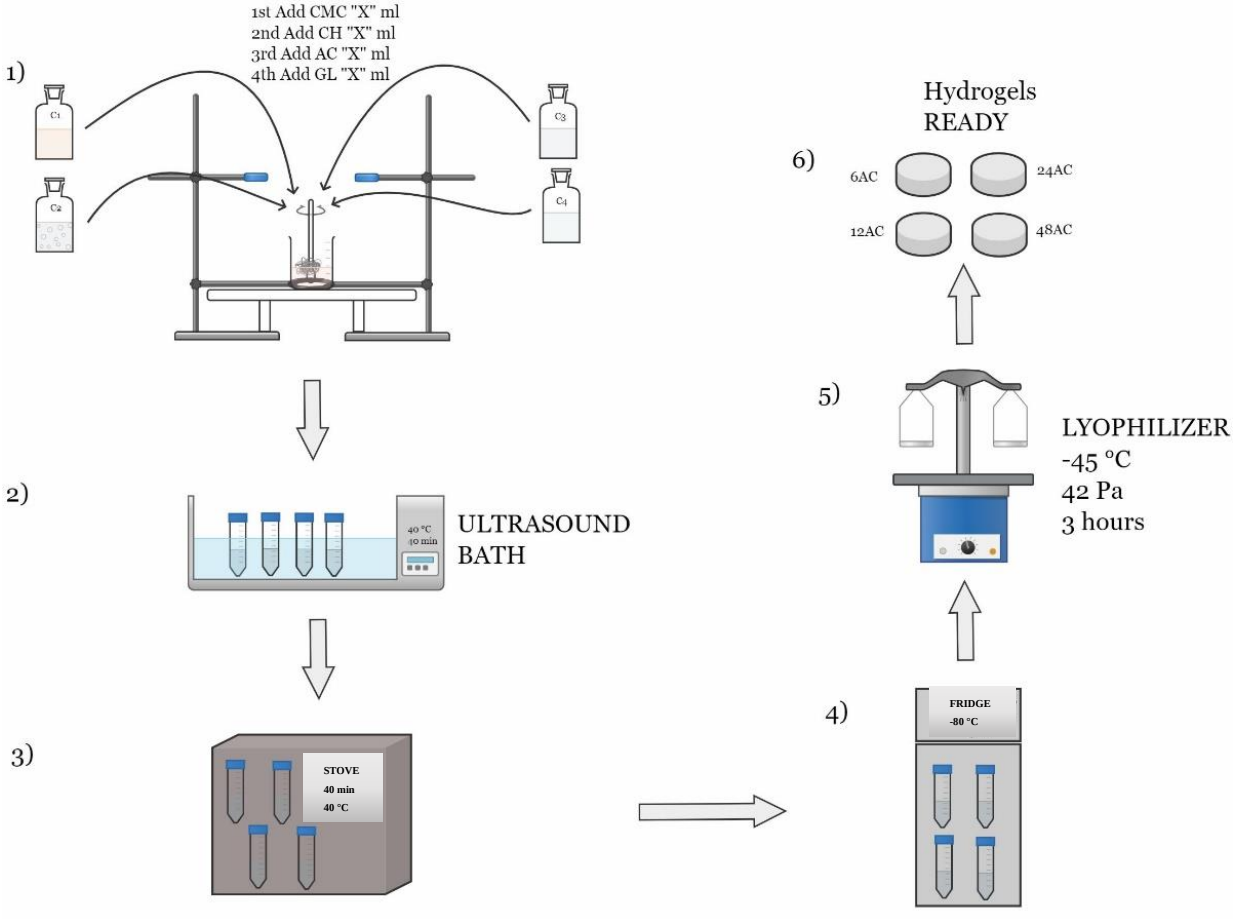

Figure 14. Scheme of processes performed in the second stage of synthesis.

3.2.3 Third Stage: Physical – Chemical, characterizations.

See below in a schematic that was prepared with the different types of hydrogels already created. See in Figure 15.

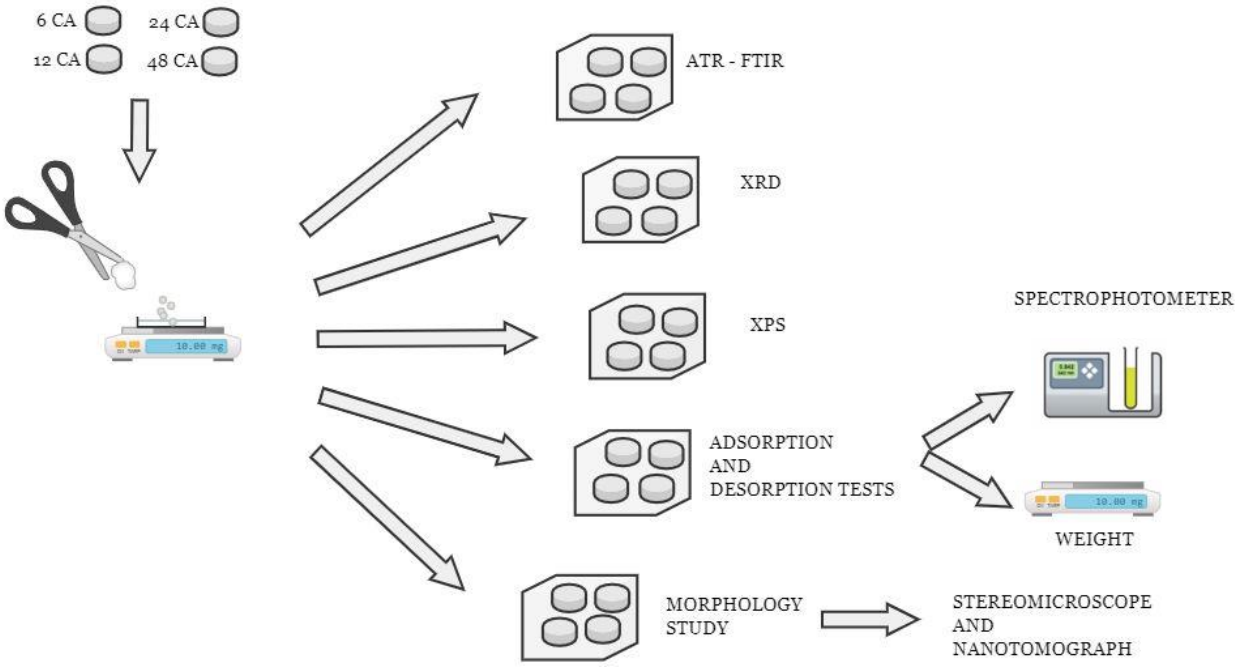

Figure 15. Scheme of hydrogel's processes performed in the third stage

3.3 Physicochemical Characterization Techniques

The techniques used to characterize the synthesized hydrogel were: Attenuated Total Reflection – Fourier Transform Infrared Spectroscopy (ATR-FTIR), X-Ray Diffractometry (XRD), X-Ray Photoelectron Spectroscopy (XPS), Morphology Study, and Swelling Study.

3.3.1 Attenuated Total Reflection FTIR Spectroscopy (ATR-FTIR)

It was allowed to know the functional groups containing the hydrogel in its crossover chain; these data were studied by FTIR using a Cary 630 with 1-Bounce Diamond ATR accessory. The spectra were obtained in the range of 4000–400 cm^{-1}, with a spectra resolution of 4 cm^{-1} and 32 scans.

3.3.2 X-Ray Diffraction (XRD)

The crystalline structure of hydrogels was studied by X-Ray powder diffractiont: A Mini-flex-600 from Rigaku, with a D/tex Ultra 2 detector. The X-Ray generator, Ni-filtered Cu Kα radiation (λ = 0.15418 nm), was fixed at 40 kV, 15 mA. For collecting data, powder samples were placed on a glass sample holder, and the selected angular region was 2θ = 5°-90° with a step width of 0.01°.

3.2.1 X-Ray Photoelectron Spectroscopy (XPS)

Analysis was performed to get chemical information on some selected CMC/CH composites hydrogels. A PHI 5000 Probe III Scanning XPS Microprobe from Ulvac phi, inc. For the sample preparation, each sample was placed onto a polymeric-based adhesive tape that was hold in a metallic mesh. High resolution deconvolution was performed using Tougaard background subtractions, and Voigtian and Gaussian functions. The software used for this purpose was Fityk and Ominic[103].

3.2.1 Morphology study

A morphology study of dried composites hydrogel was carried out in a SZX16 stereomicroscope at different magnifications (Olimpus) and nano tomography equipment was a lab-based Bruker Sky Scan 2211b; this apparatus is able to hold samples of up to 300 mm in diameter and 400 mm in height

3.2.1 Swelling Study

A dry hydrogel sample of approximately 15 mg with 10 ml of distilled water on three solutions with different pH concentrations (acid, medium and basic). Data collected was: first 5min, second in 30 min and finally every hour. The data obtained was then used in a time vs swelling graph, with equation (28) to obtain the percentage of swelling of each hydrogel.

3.2.1 Four Stage: Performance, Kinetics, and Mechanism.

3.2.1.1 Adsorption and desorption tests

3.2.1.1.1 Ultraviolet – Visible (UV-Vis) Spectrophotometry. (Adsorption evaluation)

UV-Vis spectrophotometer SPECORD S600 from Analytik Jena, with a polychromator with concave holographic grating and photodiode array (1024 pixels), with a wavelength range of 190-1100 nm ± 2 nm. The light sources used are a halogen lamp for the VIS and infrared region and a deuterium lamp for the UV region. The system is controlled by the modular software package WinASPECT. UV-Vis instrument was calibrated using standard Ce preparations from cerium sulfate (IV) in H_2SO_4 1N.

3.2.1.1.2 Kinetic batch studies on Ce (IV) adsorption

The hydrogel samples (6, 12, 24, 48 CA) were subjected to adsorption testing, containing 10 mg per sample in a 50 mL aqueous solution, the liquid medium was composed of cerium metal (100 ppm). In addition, a series of batch experiments were programmed, where 150, 160,170,180,190, or 200 mg/L of Ce (IV) solution was added to individual 250 mL (beaker or volumetric flasks) containing 10 mg of R48. All experiments were performed under ambient conditions and samples were gently shaken by hand during the measurement time, to establish adsorption equilibrium. Then, 3 mL of liquid phase of each solution obtained were added to a quartz cell, light absorbance of the samples was measured at 316 nm using spectrophotometer, and the results were used to calculate the amount of adsorption per used sorbents, at equilibrium *qe*.

3.2.1.2 Desorption Test

Experiment desorption was done with EDTA and H_2SO_4 at different concentrations, in both cases at 1M and 0.5M[48]. Between those components was evaluated the capacity to desorb of hydrogel's structure. The desorption test was in batch mode (T=24°C, t=72h). For this experiment was needed 50 mL of EDTA and H2SO4, with a weight of approximately 10 mg for each hydrogel composite. Five types of hydrogels were used, which were submerged at 100 pm cerium. To obtain of percentage of desorption in each component, we use the Equation (27).

CHAPTER IV

4. Results and Discussion

The result of the hydrogel shows in Figure 16, after having been lyophilized. Hydrogel has a porous and uniform appearance, with firm structures.

Figure 16. Synthetized compound (Hydrogel-composite).

Hydrogels was stored in hermetic containers. See in Figure 17, all types of hydrogels composites formed in this research varying the concentrations of CA.

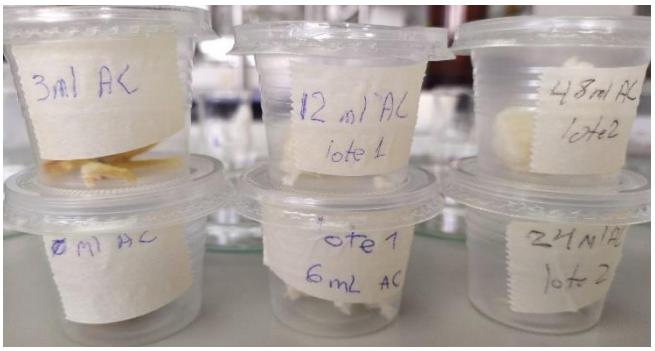

Figure 17. Hydrogels materials at different concentrations of Citric Acid.

4.1 Fourier Transform Infrared Spectroscopy - Attenuated Total Reflectance

The FTIR spectra of Hydrogel-composite, are shown in Figure 18, and a detailed assignment thereof in Table 12. All spectra were similar to each other, showing the characteristic bands of the CH and CMC.

It briefly details what can be seen in each of the observed spectra:

- The widest band can be seen in the range of 3000 - 3600 cm^{-1}; this can be attributed to the N-H stretching vibrations of free amino groups and O-H stretching vibrations. According to the theory studied, the existence of water gives this and hydroxyl; even intramolecular hydrogen bonds can be involved in this range.
- The asymmetric stretching of the C-H bonds represents the groups of -CH_2 to 2934.7 cm^{-1}. And the groups -CH_3 are at 2883.2 cm^{-1}.
- The bands between 1650 and 1610 cm^{-1} are linked C = O, known as stretching vibrations of amino acetylated groups (amide I).
- Vibration bending of the N-H and -NH_2 groups in chitosan is associated with the free amino groups in the band at 1591.6 cm^{-1}, as are the symmetrical stretching vibrations of the COO groups in the CMC. While in the 1500 cm^{-1} band, it is associated with ionic interactions or hydrogen bonds between chitosan and CMC.
- In the 1442 cm^{-1} band, the vibrations of the $NHCOCH_3$ groups occur with a slight symmetrical bending of the methylene CH_2 group. In the bands 1395.2 cm^{-1} and 1321.5 cm^{-1}, asymmetric bending of the methyl group -CH_3 occurs.
- The stretching vibrations of the CN group (amide III) correspond to the 1315 cm^{-1} band, as does the N-H stretching of N-acetyl-glucosamine.
- C-N stretching vibrations in free amino groups appear at 1207.5 cm^{-1}.
- The asymmetric group C-O-C belongs to the B-glycosidic bond and exists in the 1103.9 cm^{-1} vibration band.
- The stretching vibration of the C-O bond (ring saccharide) are found consecutively in the bands of 921.9, 1012.2, 1029.4 cm^{-1}

- The 786.8 cm^{-1} vibration band is related to the bending of the C-H group of the β-linked glycosidic bond[104,105].
- According to the literature[106–108], ester bond formation occurs in the 1730 cm^{-1} band. The presence of CMC and CA produces the esterification reaction. In addition, a different intensity was observed for each type of CA hydrogels, which is given by the degree of chemical reticulation.

a)

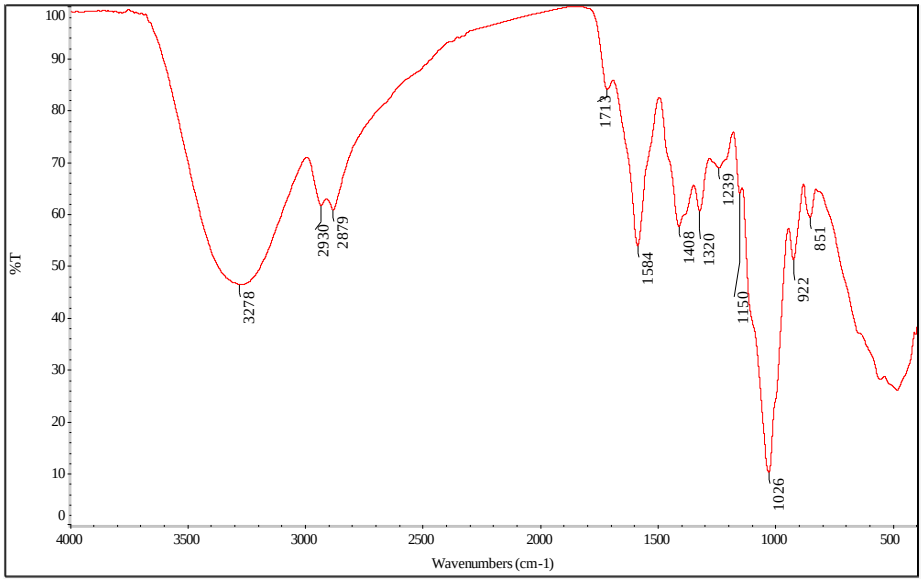

b)

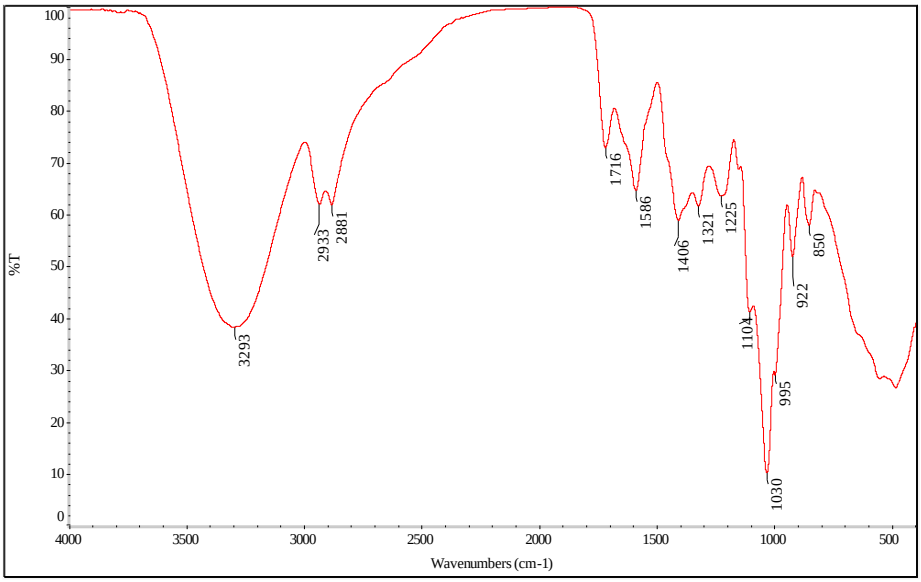

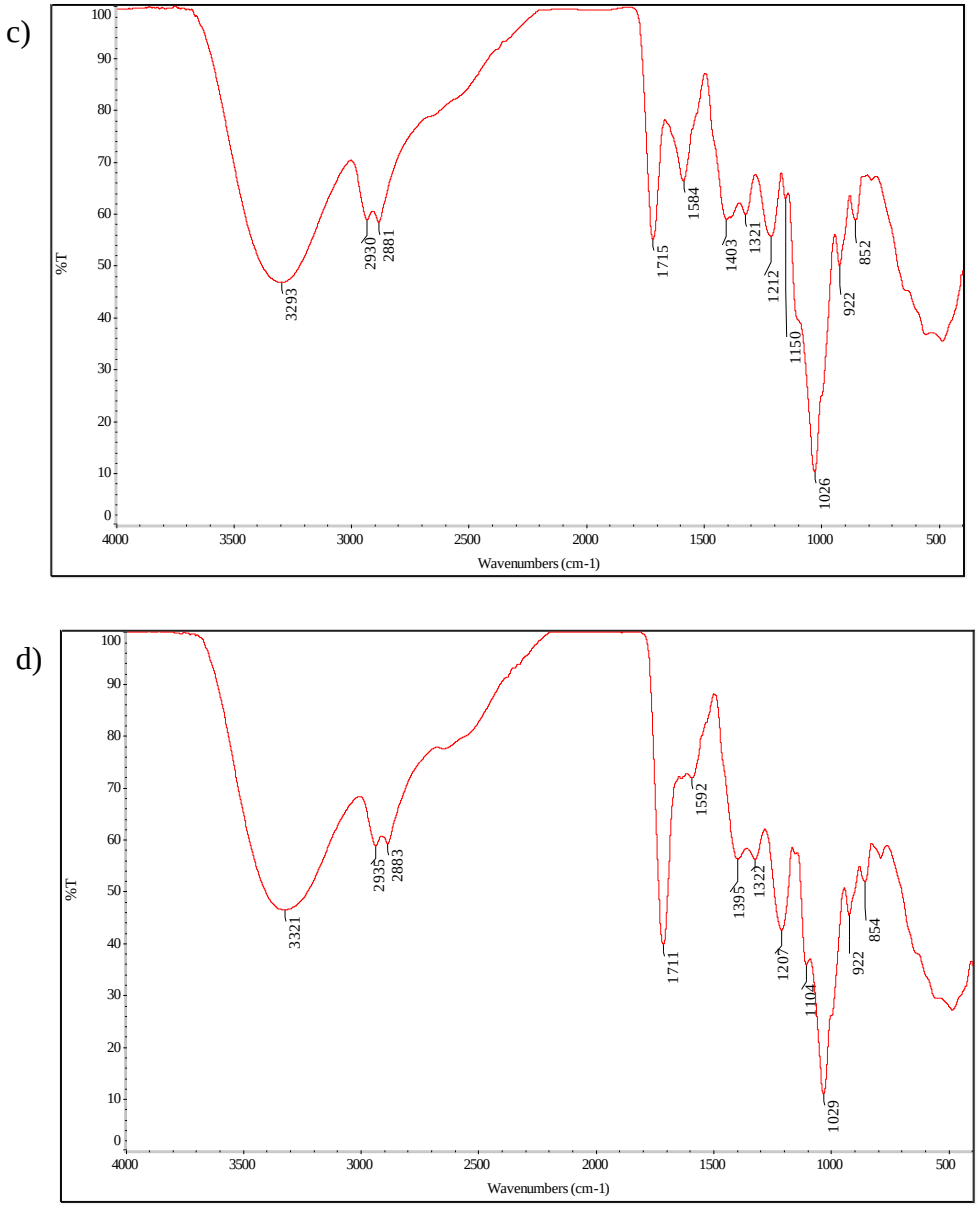

Figure 18. FTIR - Types of hydrogels at different concentrations of CA. a) 6, b) 12, c) 24, d) 48.

Table 12. FT-IR assignment for spectra vibrations CH.

Wavenumber (cm^{-1})	**Vibration type**	**Assignments**
3600-3000	v O-H, v N-H	N-H stretching Vibration of free amino groups O-H stretching Vibrations of water and hydroxyls as well as – intramolecular hydrogen bonds
2919	v_{as} C-H	CH_2 in CH_2OH group
2862	v_s C-H	CH_3 in $NHCOCH_3$ group
1722	v C=O	C=O ester
1651, 1640	v C=O	acetylated amino groups (Amide I)
1584	δ_{ip} N-H	free amino groups
1565	δ N-H v C-N	N-acetylgroup (Amide II)
1462, 1419	δ_{ip} C-H (CH_2) δ_{as} C-H (CH_3)	CH_2 in CH_2OH group CH_3 in $NHCOCH_3$ group
1375	δ_s C-H (CH_3)	Bending vibrations of methyl in $NHCOCH_3$ group
1319	v C-N v N-H	C-N (amide III) and N-H stretching of N-acetyl-glucosamine
1261	v C-N	Free amino groups
1207	v C-O	C-O ester
1149	v_{as} (C-O-C)	β -glycosidic link C-O-C (bridge)
1059	v (C-O)	C-O ring saccharide structure
1023	v (C-O)	C-O ring saccharide structure
987	v (C-O)	C-O ring saccharide structure
892	δ C-H	β-linked glycosidic bond

Taken from Wojdyr[103] and Ibitoye[104].

The vibration band definitions in the IR spectra have been collected, the four graphs, 6AC, 12AC, 24AC, and 48AC. Due to the values obtained in the vibration bands and the peaks presented in Figure 19, it can be indicated that the compound hydrogels have a uniform structure with functional

groups such as amines, among others, which are excellent for the absorption of heavy metals in aqueous media[109].

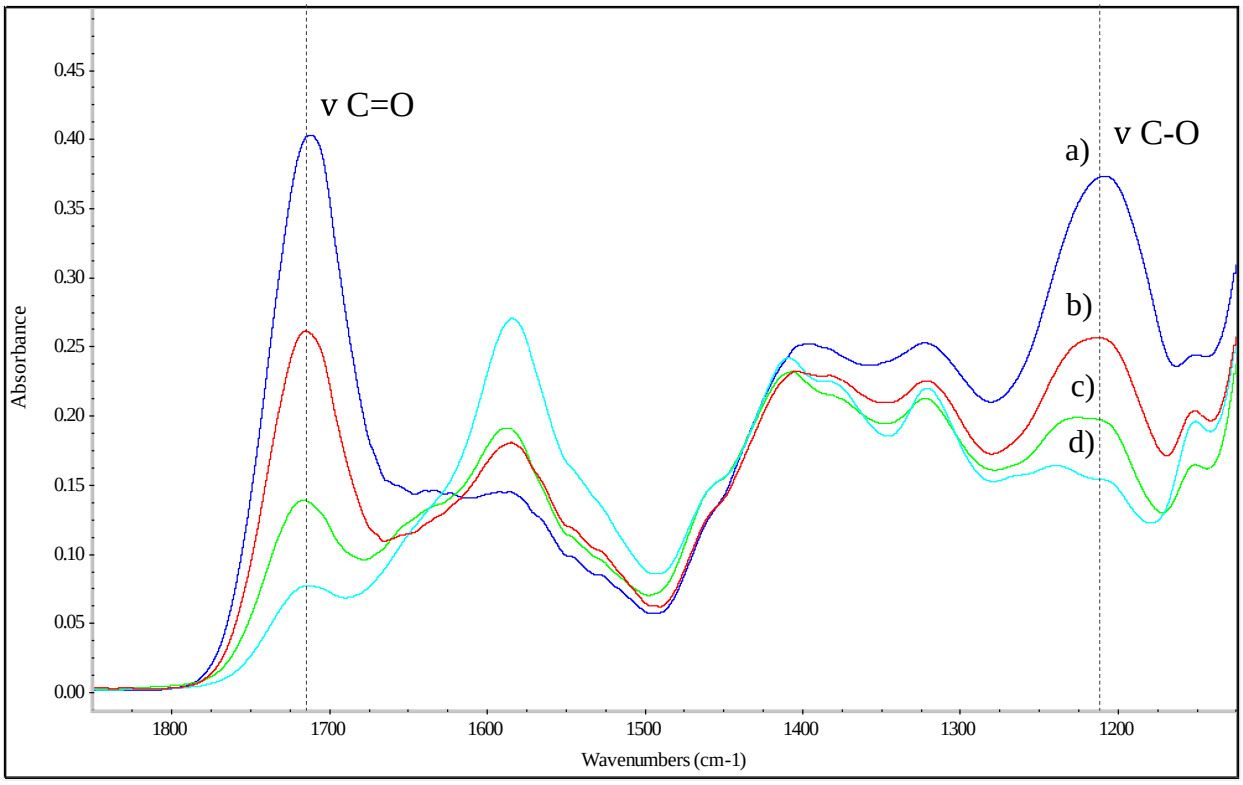

Figure 19. FT-IR. Enlargement region 1850-1125 cm^{-1}. a) blue 48 CA, b) red 24 CA, c) green 12 CA, d) 6 CA.

4.2 X-Ray Diffractometry (XRD)

The X-ray diffraction pattern of the hydrogels are illustrated in Figure 20. As we can see in the crystalline peak width to $2\theta \approx 21.6$ °, the characteristics of the diffraction suggest that hydrogels are highly amorphous, due to cross-linking.

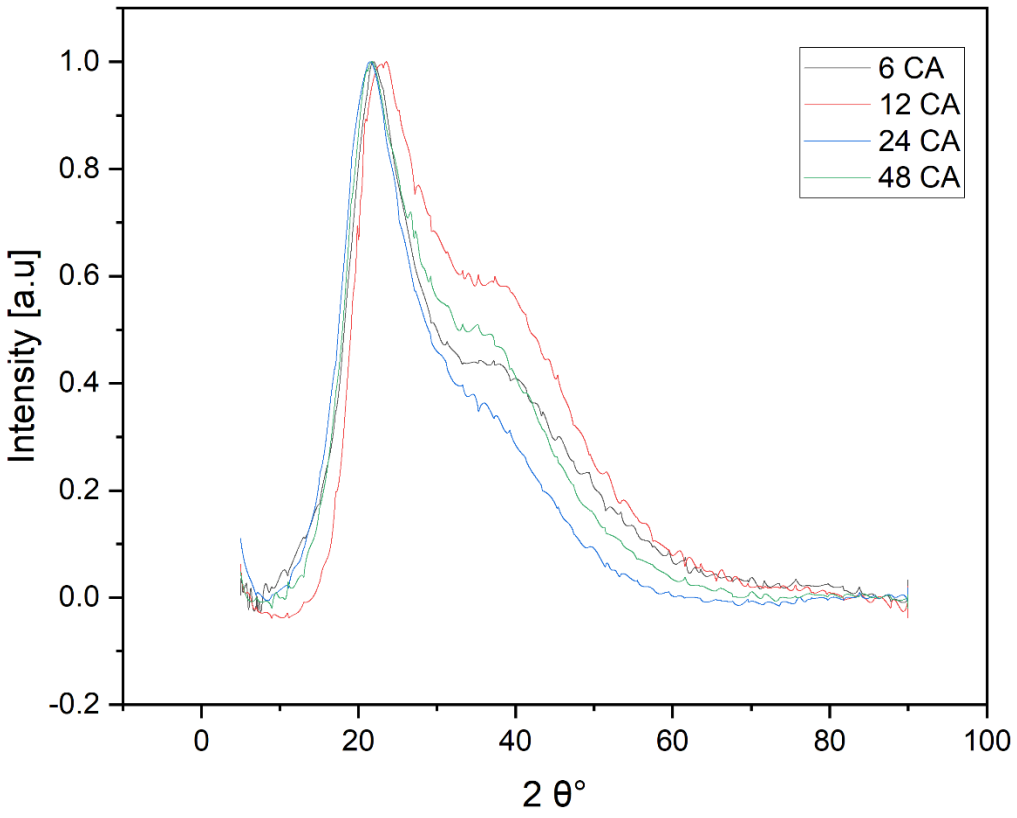

Figure 20. Fig. XRD – Patterns at different concentrations of CA. a) gray 6, b) red 12, c) blue 24, d) green 48.

4.3 X-Ray Photoelectron Spectroscopy (XPS)

Figure 21 shows the high-resolution spectra C1s of hydrogels composite. The peaks found are listed below[103,104]:

- 284.3 – 284.923 (eV) represents links -CC - / - CH
- 286.415 (eV) represents links -CN - / - CO - / -COH
- 287.809 (eV) represents links -C = O / -OCO - / - NC = O /-C N
- 288.95 (eV) represents links - COO− / -COOH

The signal associated with COOH and CO groups increments with higher concentratios of CA, which confirms the incorporation of CA into the hydrogel matrix

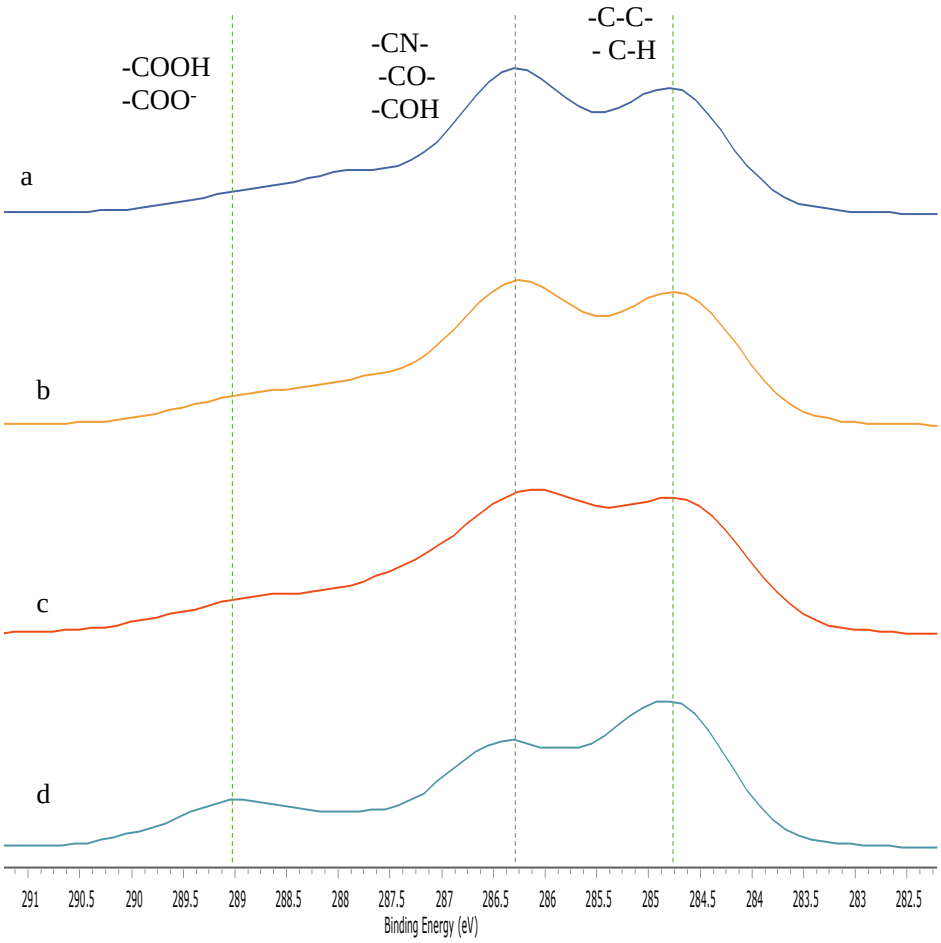

Figure 21. survey XPS HR 1Cs – Spectra in range 280 to 300 eV.

The high-resolution spectra N1s of hydrogel composite, Figure 22, show two peaks at 400.00 eV and 401.775 eV associate to bonds -NH_2 and -O-C-N, and NH_3^+ respectively. The increment of the signal at 401.775 eV with CA concentration is due to the formation of ionic crosslinks between -NH_2 groups from CH and COOH groups from CA and CMC, by ion interactions, or hydrogen bonds[110].

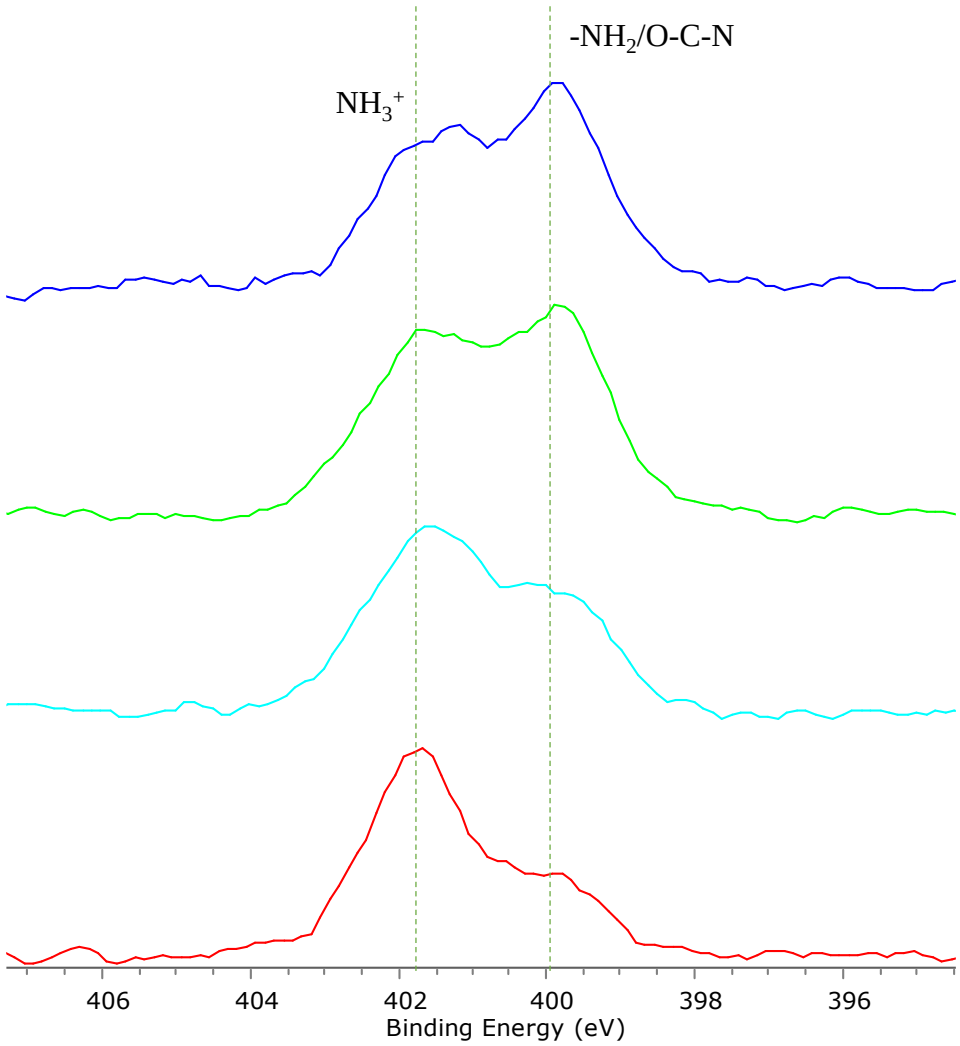

Figure 22. survey XPS HR – Spectra in the range 394 to 408 eV(N1s).

4.4 Adsorption and desorption tests

4.4.1 Ultraviolet – Visible (UV-Vis) Spectrophotometry. (Adsorption evaluation)

For the kinetic study of the Ce metal (IV). Samples of 6, 12, 24, and 48 AC in 100 Ce ppm were studied to find the type of hydrogel with a more robust adsorption capacity than other samples. During the experimental test, 6 AC sample had to be discarded because the sample disintegrated; thus, the adsorption vs. time curve could not be completed. For the other hydrogel samples, the curve is shown in Figure 23. After obtaining the results, we realized that the hydrogel of 48 mL

CA has an excellent absorption capacity so much that we could consider it a robust absorber. For this reason, we worked on the kinetic study with 48 mL at different concentrations of cerium ppm and also, we use kinetic models for adsorption isotherms.

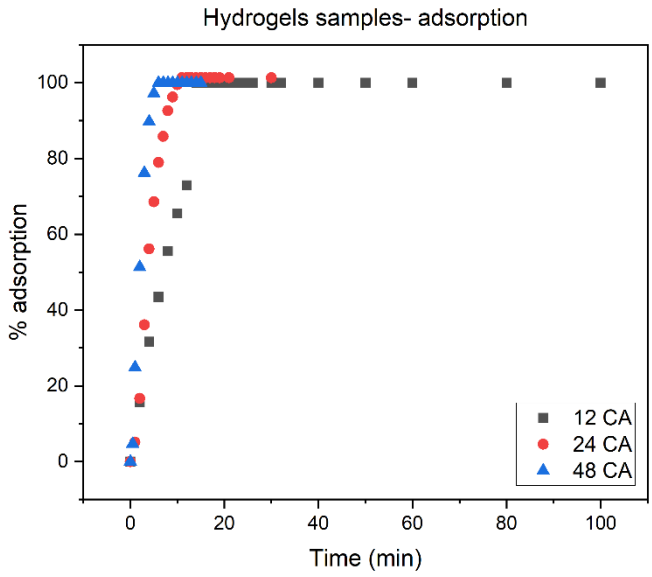

Figure 23. Adsorption graph for different hydrogel samples.

Figure 24, present the adsorption kinetic of 200 mg L^{-1} aqueous solutions of Ce (IV) onto 5 mg of 48 CA material. It can be seen that Ce (IV) rapidly adsorbed onto 48 CA, and reached equilibrium after ~10 min.

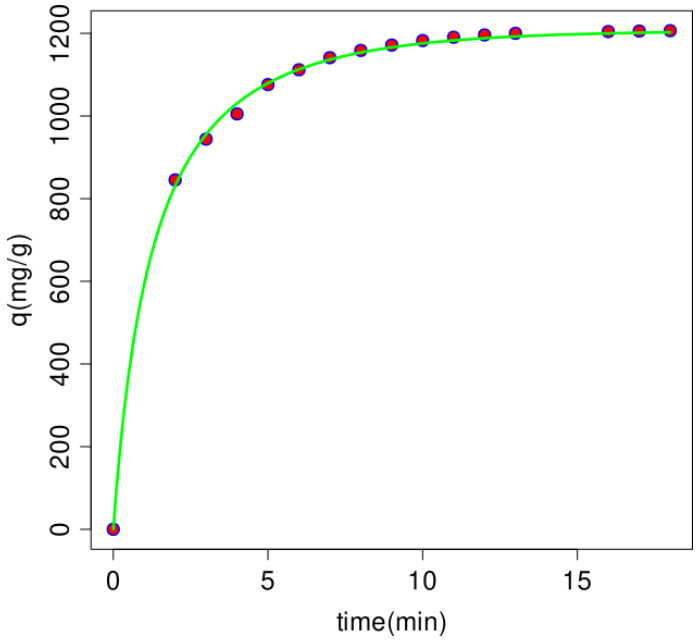

Figure 24. Kinetic study of 48 CA – hydrogel composite.

All the data was analyzed by solving the kinetic models considered through a script written in R. To evaluate the performance of the kinetic models, the residual standard errors (RSE) were calculated and compared, and residual graphs were plot and analyzed. The best fit of data was reached using the mixed order model (MO). A summary of the kinetic parameters obtained for Ce (IV) concentrations of 150, 160, 170 ,180 ,190, and 200 ppm, using MO model is presented in Table 13.

Table 13. summary of the kinetic parameters obtained for Ce (IV) concentrations of 150, 160, 170 ,180 ,190, and 200 ppm.

Initial Concentration (mg L^{-1})	$q_{e,\,exp}$ **(mg g^{-1})**	$q_{e,fit}$ **(mg g^{-1})**	k_1 **(min^{-1})**	$k_2 \times 10^{-4}$ **(min^{-1})**	**RSE (22 df)**
150	~ 1352	1372 ±10	0.16 ±0.01	3.3±0.1	9.98

160	~ 1490	1491±10	0.09±0.01	1.0±0.1	7.72
170	~1523	1518±07	0.09±0.01	1.0±0.1	5.11
180	~1600	1588±11	0.03±0.01	1.0±0.1	6.05
190	~1595	1598±10	0.03±0.01	1.0±0.1	5.92
200	~1597	1605±10	0.025±0.01	5.0±0.1	3.25

MO model is a hybrid kinetic equation, with a lineal combination of Pseudo first order (PFO) and Pseudo second order (PSO) models. For some systems, PFO and PSO models only describe the initial and final conditions in the overall adsorption process. PFO model can describe the initial stage of adsorption, when a few adsorbent active sites are occupied, while the PSO model represents the end stage of adsorption, when most of the active sites are occupied. In those situations, the MO model represents the overall adsorption process. Furthermore, the MO model can represent any stage of the adsorption process, especially when the diffusion of adsorbate and/or the adsorbate adsorption onto the active sites is the dominant step in the mass transfer adsorption process. It is valid at arbitrary initial adsorbate concentration in solution. The MO model, being a differential equation, was solved by using 4–5 order Runge-Kutta method. The values of the pseudo-first-order rate constant k_1 of the MO model range between 0.09 and 0.025 min^{-1}; and the values of the pseudo-second-order rate constant k_2 were between 1 to 5 $\times 10^{-4}$ g/(mg·min), respectively, implying that the adsorption is the combination of the pseudo-first- and -second-order kinetic processes.

The rate of the overall adsorption process could be calculated using the equations:

Pseudo-first-order-rate = $k_1(q_e - q_t)$; Pseudo-second-order-rate = $k_2(q_e - q_t)^2$

The rate of the overall process is shown in Figure 25. We can see that the PFO rate (the rate of external diffusion) was in the same order of magnitude as PSO rate (the rate from adsorption at active sites), indicating that the adsorption process was dominated by multiple rates limiting steps. Highest values of the PFO and PSO rate were achieved at the beginning of the adsorption process, and decreasing quickly with time until equilibrium.

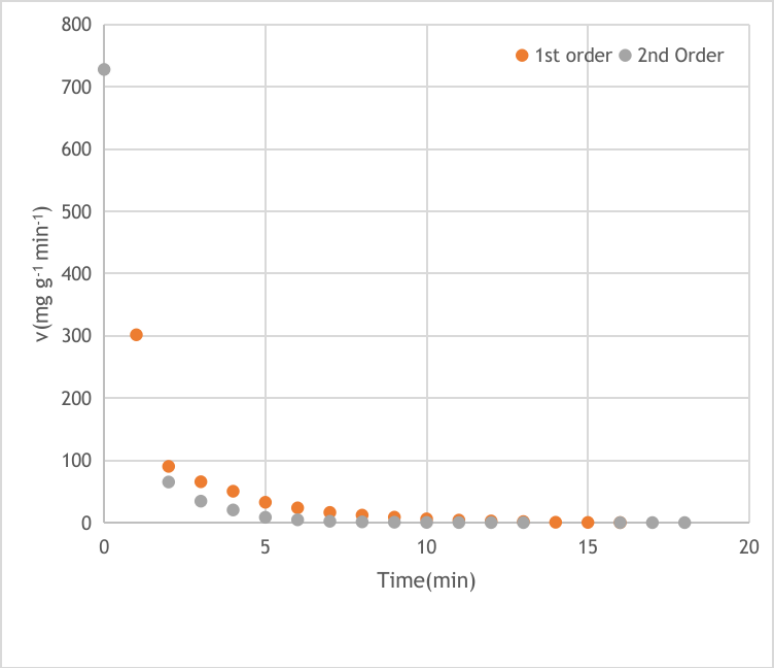

Figure 25. The overall adsorption rate of the kinetic data from Ce (IV) 200 ppm solution adsorption onto 0.5 mg of 48 CA.

4.4.2 Desorption Test

After Ce (IV) adsorption, hydrogels-composite were treated with desorption agents (EDTA and H2SO4). In the following Table *14*, we find the results for each type of hydrogel.

Table 14. Desorption efficiency (%).

Type of Hydrogel	**Reagent**			
	EDTA 0.1M	EDTA 0.05M	H_2SO_4 0.1M	H_2SO_4 0.05M

6 CA	40.8	35.6	33.5	21.2
12 CA	42.2	35	39.7	26.4
24 CA	55.7	41.6	46.3	24.1
48 CA	78.5	56.8	48.2	38.3
48 CA (NL)	22	21.2	19.2	16.2

The best desorption agent is EDTA 0.1M, with a percentage of 78.5% for the 48 CA sample. While the worst sample is for H2SO4, 0.05M the value of 16.2% for the 48 CA (NL), the closest reason may be because it did not receive lyophilized treatment. According to Pietrelli, L[48] et al., EDTA is a hexadentate chelating agent capable of forming a stable complex with heavy metal ions such as Ce (IV).

4.5 Morphology Study

The morphology of the hydrogels-composite is shown in Figure 26 and Figure 27. It was observed trough the nano tomograph and stereomicroscope. In nano tomograph a) and b) the chains of the hydrogel structure have a heterogeneous porous distribution. In addition, there is a presence of macropores, and there is no visible porous interconnectivity.

Also, there is roughness samples, and this is due to the presence of intermolecular hydrogen bonds between CMC and CH[109].

a)

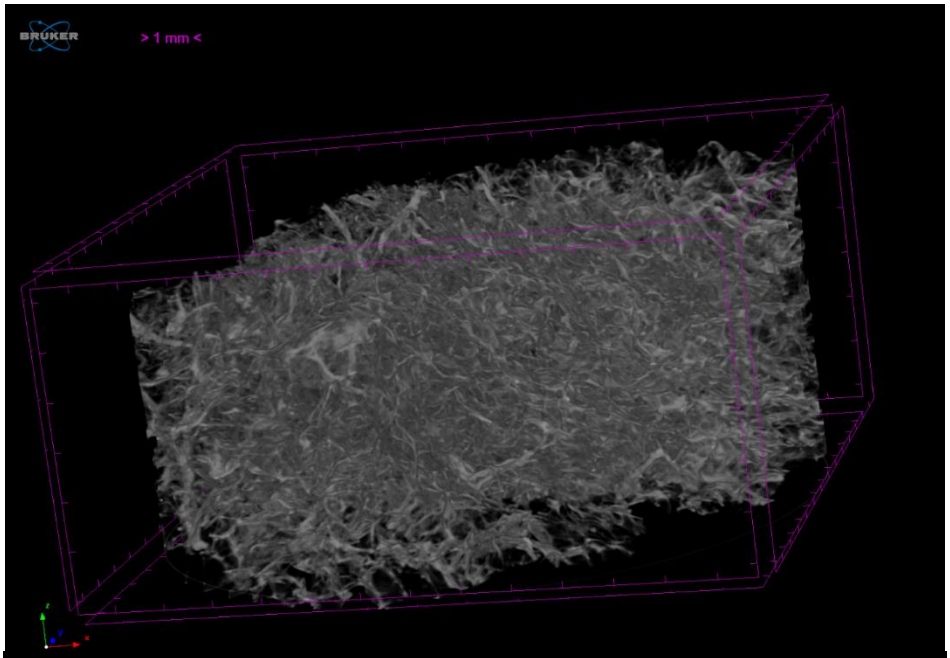

b)

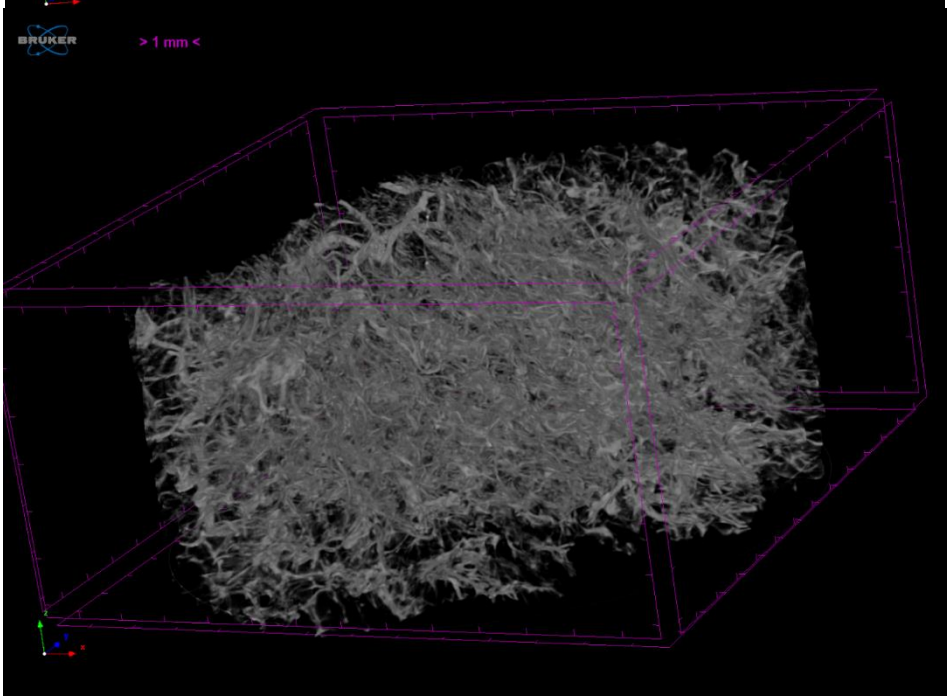

Figure 26. Hydrogels ramifications at different concentrations of citric acid. a) 48 CA; b) 6 CA. Photographs by the nano tomograph.

In stereomicroscope, spherical cavities could be observed. According to theory[111]:

- The structure has electrostatic interactions between polymer molecules, and there is chain formation. Spherical cavity represents surface action and agitation force.
- Spheres cavities can be filled with water or any liquid substance, increasing their weight. The hydrogel can return to its natural form once there is evaporated occur. Verified with desorption tests, it does not damage the structure, and it regenerates after drying completely.

a)

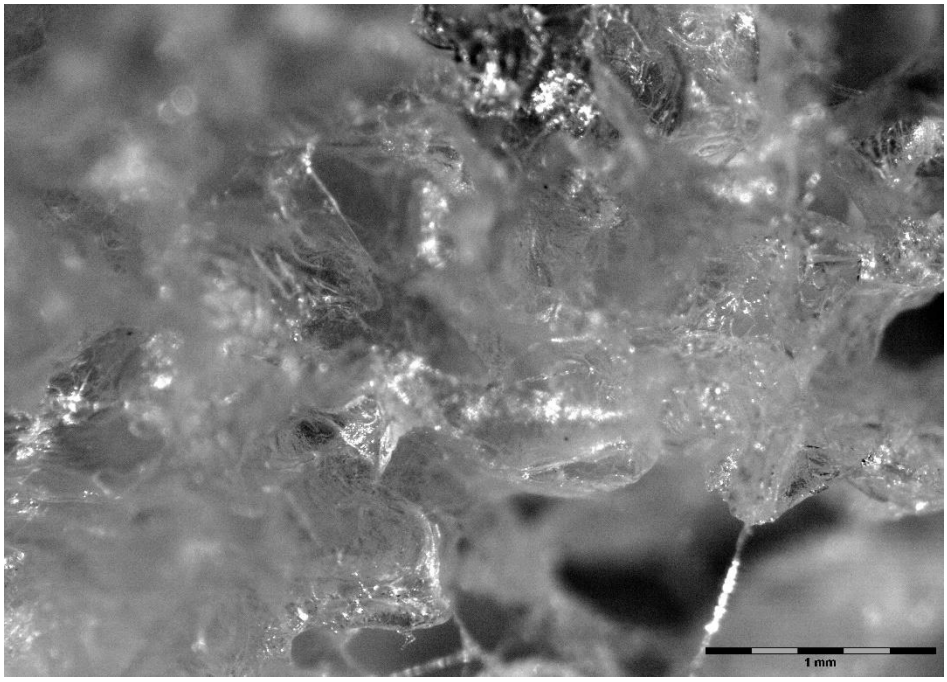

b)

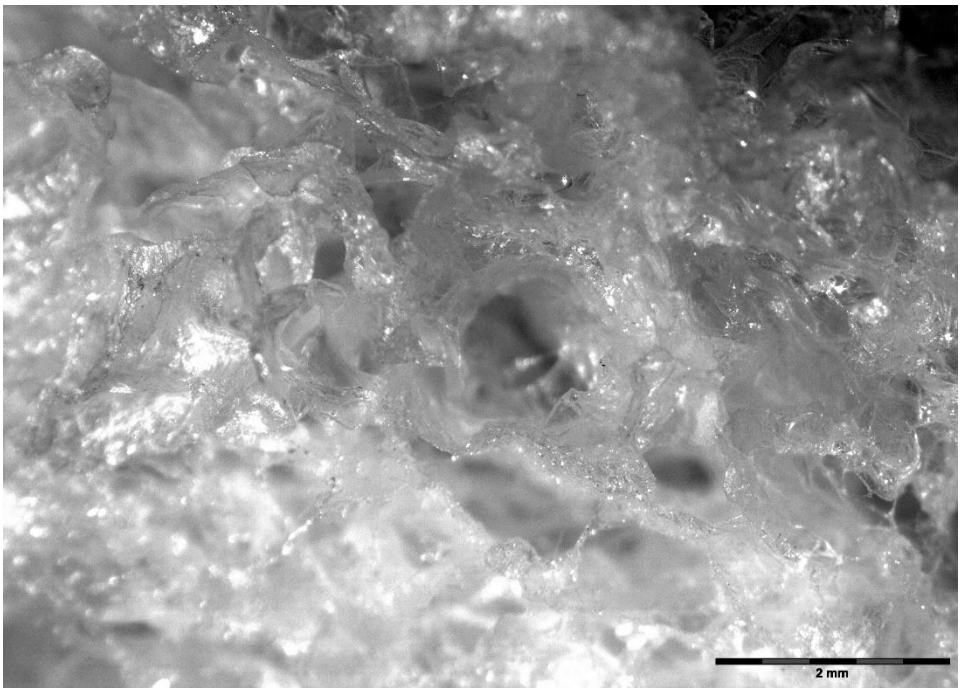

c)

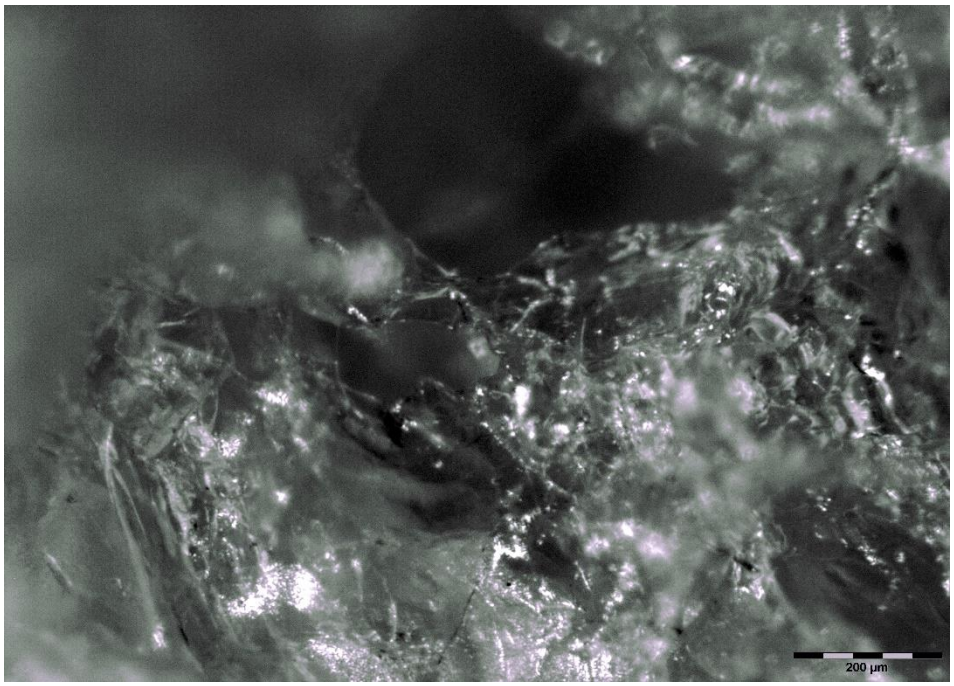

d)

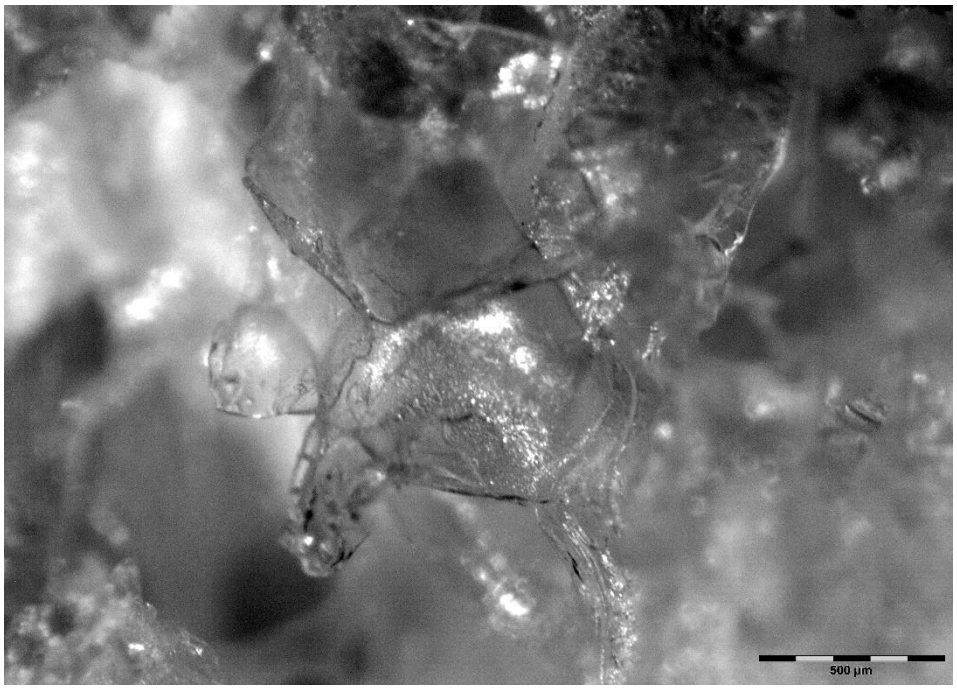

Figure 27. Structure of the hydrogel at different magnifications. a) 1 mm, b) 2 mm, c) 200 µm, d) 500 µm Photographs by stereomicroscopy.

4.6 Swelling Study

This test was performed to determine the absorption capacity in different media solution. The acid, neutral, alkaline solutions were used. In Figure 28, shows the swelling ratio vs time.
After having performed the swelling tests on each type of hydrogel. It was reported that:

- The shape of the hydrogel-composite changed rapidly at 6 mL CA.
- The hydrogel presented peculiar characteristics such as flexibility, softness, and fragility.
- In the acid medium (pH 3); the hydrogel structure tends to disintegrate due practically to the lack of hardness in the reticular walls. Disintegration occurred in 6 mL AC hydrogels, while 12 mL AC or more hydrogels are suitable for acid media. The hydrogels of 6 mL AC at pH 7 achieved a tremendous swelling; this happens basically by the junctions of the

bonds that can be stretched; therefore, not having enough chemical reticulation in their structure, the capacity of swelling increases. See in Figure 29.

a)

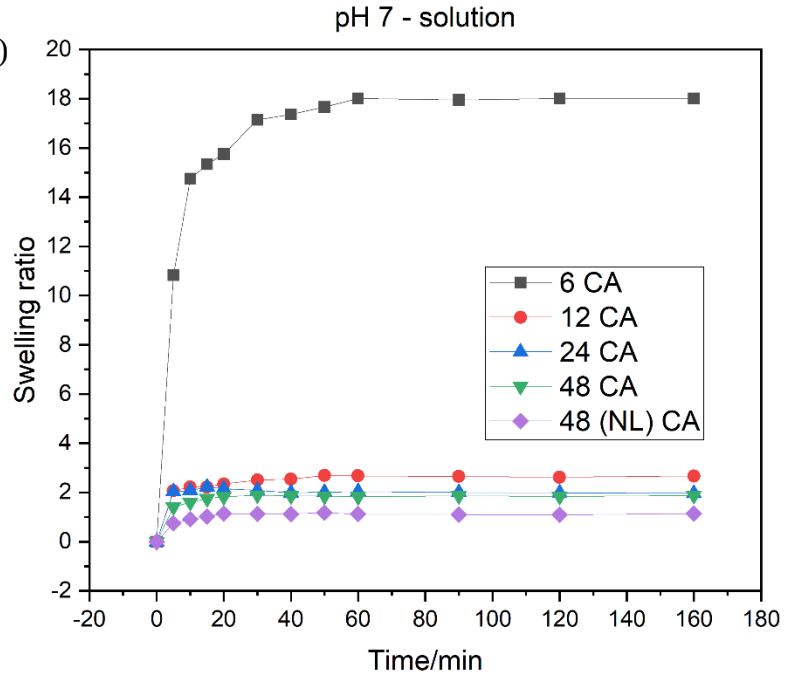

b)

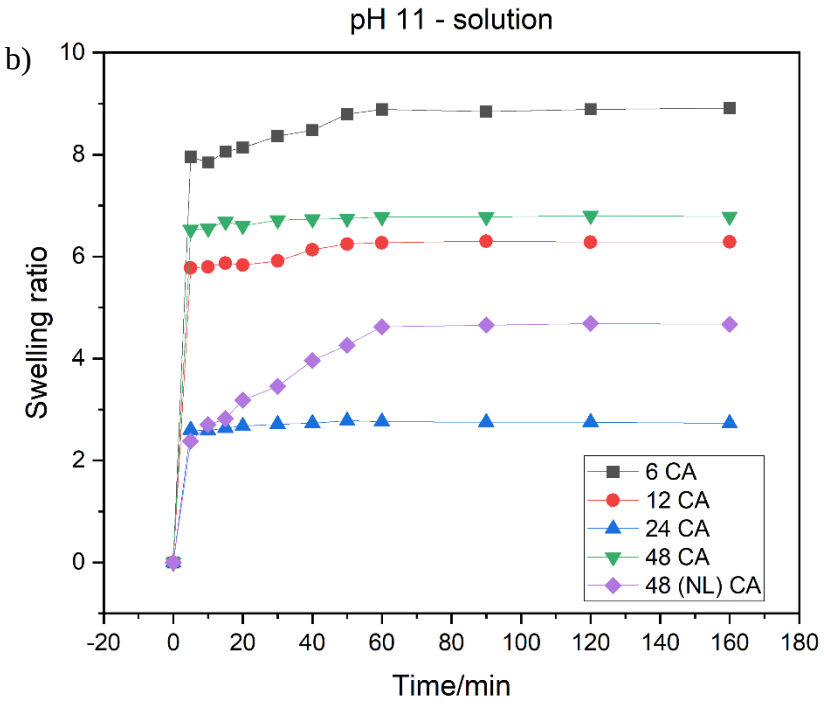

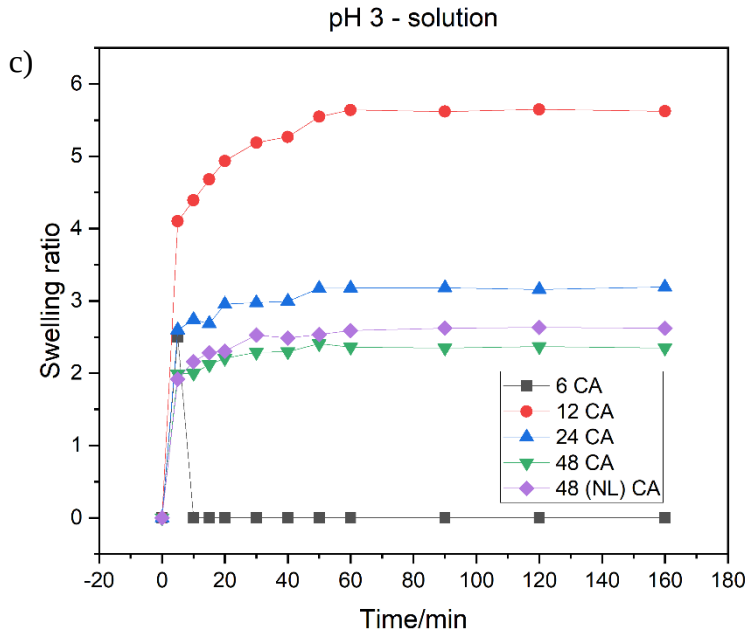

Figure 28. Swelling ratio vs time of hydrogels-composite prepared with CMC/CH/AC/GL at different ratio of Citric Acid. a) neutral, b) alkaline, c) acid.

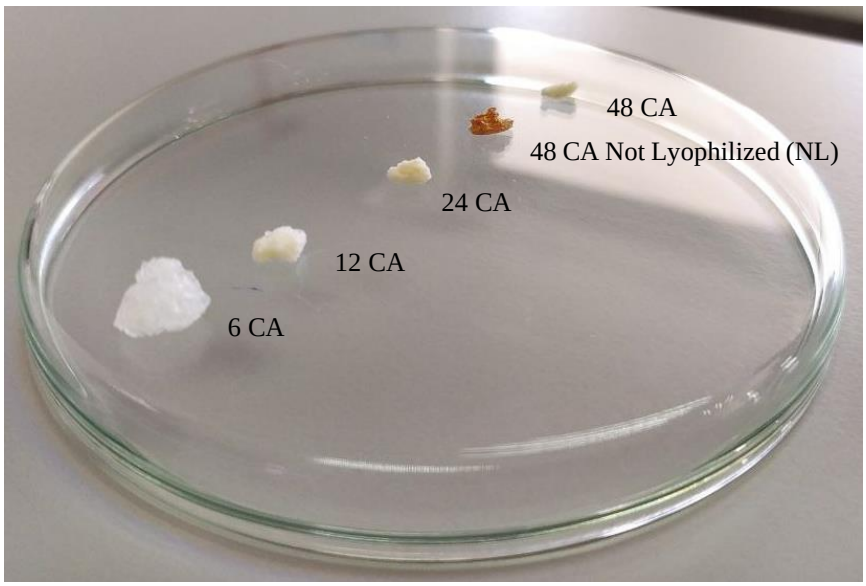

Figure 29. Types of hydrogels-composites after swelling test (pH 7 - media).

4.7 Hydrogel – Composite Overall Results

Based on the different chemical characterizations carried out, where chemical and physical cross-linking was confirmed. We are proposing an average chemical structure of the composite hydrogel. Figure 30 illustrates a proposed reaction equation of the composite hydrogel´s formation.

The groups formed were: amines, ester, hydrogen bond, ionic bond, alcohols, amides. Representative characteristics have been identified concerning the formation and structure of the hydrogel supporting the proposed mechanism;

- In the XPS, increase of NH_3^+ bond groups. The reason could be attributed to ionic cross-forming between the chitosan amine protonate group and the CMC or citric acid [110,112]. In addition, ester bonds between CMC and Chitosan can be formed with cross-linking.
- Ionic and Hydrogen bond: According to Table 12 FTIR assignments, the signal shown at 1587.64 cm^{-1} represents the bending vibration of NH groups in the chitosan. The signal also represents stretching vibration for COO- groups in the CMC. The signal 1576 cm^{-1} represents the physical interaction between COO and NH_3^+ groups between CMC and CH, respectively[109,112]. For this reason, there is an ionic interaction and hydrogen bridge in the formation of the hydrogel composite.
- Ester bond: According to Table 12. The signal at 1716.7 cm^{-1} results in the formation of ester bonds. And suggests that the bond of ester is forming in CMC and CA[106–108,113].

1)

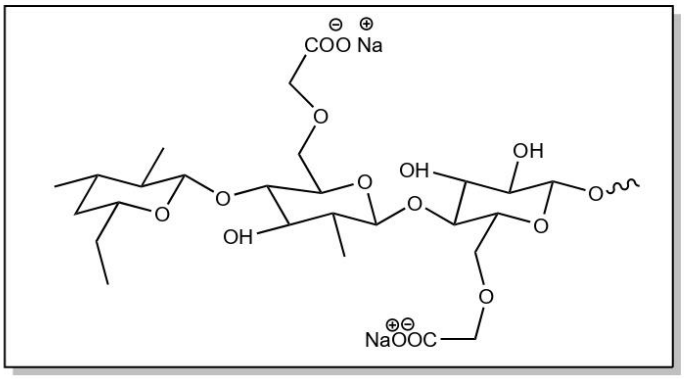

Carboxy methyl cellulose

2)

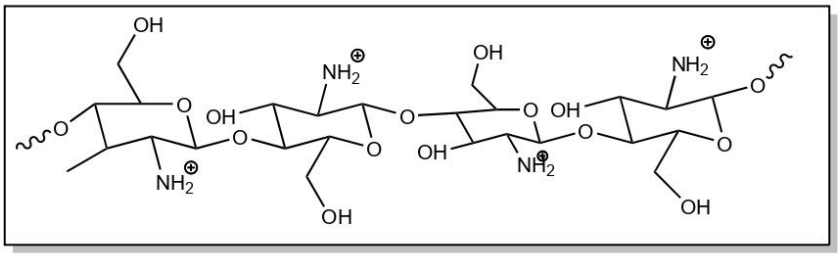

Cross-linked Chitosan

3)

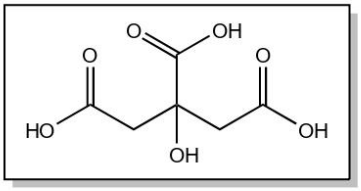

Citric Acid

4)

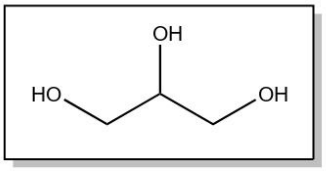

Cross-linked Chitosan

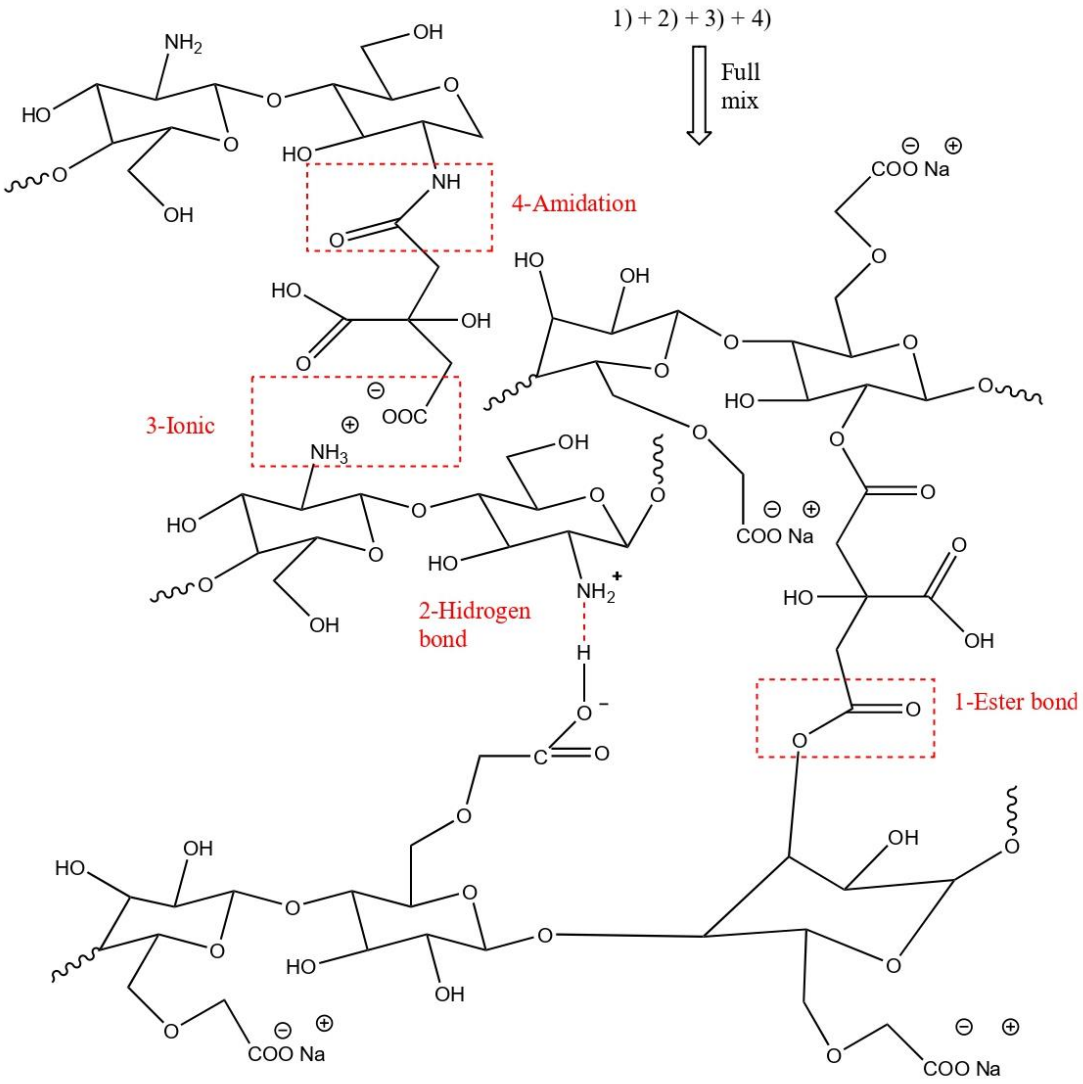

Figure 30. Reaction equation of the composite's hydrogels formation[102]

CHAPTER V

5. Conclusions and Recommendations

5.1 Conclusions

- Several hydrogels samples were prepared at different concentrations of citric acid. (6, 12, 24, 48 AC). Due to the lyophilization process, increased adsorption capacity and chemical reticulation.
- Depending on the citric acid concentrations, the hydrogel-composite varies its application. Citric acid is an effective crosslinker promoting the formation of amide and ester bonds between CMC and CH compounds. Moreover, hydrogel structure has a heterogeneous porous distribution and there is a presence of macropores.
- The swelling capacity increased in the neutral pH 7 (neutral), while in pH 3, 11 medium; there is a reduced capacity of the hydrogel.
- The hydrogel-composite quickly absorbs Ce metal under standard conditions and within about 10 to 30 min; depending on the concentration of Ce (ppm). The hydrogel with the highest absorption capacity was 48 mL CA lyophilized, so it was concluded that the more amides groups are formed, the absorption will increase. Although the capacity of swelling of the hydrogel is reduced, it is urged to carry out an upcoming research study, coming to cross other materials similar to glycerol and citric acid; in this way, compare both characteristics.
- A hydrogel sample Non-lyophilized (NL) was used to enhance the present investigation and was not freeze-dried. This hydrogel (NL) was used to compare the absorption capacity against hydrogels that did have lyophilization and varying the composition of citric acid. In summary, lyophilized compounds were much more effective than the non-lyophilized sample, so it is recommended to freeze the final product because it adds specific characteristics such as pore distribution, increased interconnectivity, among others. Hydrogels of 0;3 mL CA, these kinds of hydrogels do not have amino groups that help to capture cerium molecules.

5.2 Recommendations

- Hydrogel-composite is not created only to absorb heavy metals in aqueous media. The hydrogel could be helpful in industries such as medicine, biomedicine, and food. Therefore, it is recommended to do experiments in these fields.
- It is recommended that the following studies concerning the absorption of heavy metals in aqueous media be made an economic study. It covers from the purchase of the raw material until the export of the product. In this way, it will be known how the creation of hydrogel at the global level will impact the economic aspect.
- In the field of research, this type of combination of hydrogel does not exist, so it is highly recommended to analyze this document in depth because the absorption capacity of this hydrogel-composite could remove metals such as Hg(mercury), Pb(lead), among others.
- Kinetic studies showed excellent absorption capacity in aqueous media with pH 7. Therefore, it is recommended that several solutions with different pH should also be used in future research. In the swelling test, the hydrogel increased its weight sharply in different media (pH). Therefore, a balance must be found in which the maximum absorption capacity of the hydrogel and the maximum elasticity capacity can be achieved.

Last but not least, the implementation of this type of water treatment could serve mainly for drinking water processing plants since it was tested in distilled water with a pH 7. Suppose you want to use hydrogel in a country like Ecuador in the different municipalities. In that case, you should do a thorough study, looking at the advantages and disadvantages that it entails for society.

REFERENCES

(1) Ahmed, E. M. Hydrogel: Preparation, Characterization, and Applications: A Review. *J. Adv. Res.* **2015**, *6* (2), 105–121. https://doi.org/10.1016/j.jare.2013.07.006.

(2) Aly, O. M.; Faust, S. D. *Adsorption Processes for Water Treatment*; 1987. https://doi.org/10.1016/c2013-0-04267-3.

(3) Foo, K. Y.; Hameed, B. H. An Overview of Landfill Leachate Treatment via Activated Carbon Adsorption Process. *J. Hazard. Mater.* **2009**.

(4) Sreejalekshmi, K. G.; Krishman, K. A.; Anirudhan, T. . Adsorption of Pb(II) and Pb(II)-Citric Acid on Sawdust Activated Carbon: Kinetic and Equilibrium Isotherm Studies. *J. Hazard. Mater.* **2009**, *1* (161 (2-3)), 1506–1513.

(5) AWWA. *Water Quality and Treatment*, 4th ed.; McGraw-Hill Book Co.: New York, 1990.

(6) Pedden, T. M. *Drinking Water and Ice Supplies and Their Relations To Health and Disease*; The Knickerbocker Press: New York, 1981.

(7) United Nations Water https://www.unwater.org/world-water-development-report-2020-water-and-climate-change/ (accessed May 25, 2021).

(8) Sanjay, K. S. *Heavy Metals in Water*; The Royal Society of Chemistry: Cambridge CB4 0WF, UK, 2014. https://doi.org/10.1039/9781782620174-FP001.

(9) Dahle, J. T.; Arai, Y. Environmental Geochemistry of Cerium: Applications and Toxicology of Cerium Oxide Nanoparticles. *Int. J. Environ. Res. Public Health* **2015**, *12* (2), 1253–1278. https://doi.org/10.3390/ijerph120201253.

(10) Yan, L.; Qian, F.; Zhu, Q. Interpolymer Complex Polyampholytic Hydrogel of Chitosan and Carboxymethyl Cellulose (CMC): **2001**, *1374* (August), 1370–1374. https://doi.org/10.1002/pi.791.

(11) Zeitoun, M. M.; Mehana, E. S. E. Impact of Water Pollution with Heavy Metals on Fish Health: Overview and Updates. *Glob. Vet.* **2014**, *12* (2), 219–231.

https://doi.org/10.5829/idosi.gv.2014.12.02.82219.

(12) Saleh, T.; Seyed, S. S.; Gholamali, A. B.; Atena, D.; Mohammed, S. Heavy Metals (Zn, Pb, Cd and Cr) in Fish, Water and Sediments Sampled from Southern Caspian Sea. *Iran. Toxicol. Ind. Heal.* **2010**, *Iranian To* (10), 649–656.

(13) Wan, X.; Wang, J. Y.; Ye, J. H.; Wang, P.; Zhan, Z. M. Analysis of Distribution and Contents of Heavy Metals Pollution in Fish Body with Laser-Induced Breakdown Spectroscopy. *NCBI* **2013**, *33* (1), 206–209.

(14) Gabriel, O. M.; Rita, O.; Clifford, A.; Kennedy, O. Heavy Metal Pollution of Fish of Qua-Iboe River Estuary: Possible Implications for Neurotoxicity. *Int. J. Toxicol.* **2006**, *3* (1), 1–6.

(15) Fakhre, N. A.; Ibrahim, B. M. The Use of New Chemically Modified Cellulose for Heavy Metal Ion Adsorption. *J. Hazard. Mater.* **2018**, *343*, 324–331.

(16) Sakulthaew, C., Chokejaroenrat, C., Poapolathep, A., Satapanajaru, T., Poapolathep, S. Hexavalent Chromium Adsorption from Aqueous Solution Using Carbon Nanoonions (CNOs). *Chemosphere* **2017**, *184*, 1168–1174.

(17) Aka, E. C.; Nongbe, M. C.; Ekou, T.; Ekou, L.; Coeffard, V.; Felpin, F. X. A Fully Bio-Sourced Adsorbent of Heavy Metals in Water Fabricated by Immobilization of Quinine on Cellulose Paper. *J. Environ. Sci.* **2019**, *84*, 174–183.

(18) Tran, T. H.; Hirotaka, O.; Yoshiki, H.; Kazuhiro, H. Removal of Metal Ions from Aqueous Solutions Using Carboxymethyl Cellulose/Sodium Styrene Sulfonate Gels Prepared by Radiation Grafting. *Carbohydr. Polym.* **2017**, *157*, 335–343.

(19) Wang, F.; Pan, Y.; Cai, P.; Guo, T.; Xiao, H. Single and Binary Adsorption of Heavy Metal Ions from Aqueous Solutions Using Sugarcane Cellulose-Based Adsorbent. *Bioresour. Technol.* **2017**, *241*, 482–490.

(20) el comercio. El camarón alcanzó cifra récord en el 2019 en el Ecuador https://www.elcomercio.com/actualidad/camaron-record-ecuador-exportacion-

economia.html (accessed Aug 20, 2021).

(21) Erol, O.; Pantula, A.; Liu, W.; Gracias, D. H. Transformer Hydrogels: A Review. *Adv. Mater. Technol.* **2019**, *4* (4), 1–27. https://doi.org/10.1002/admt.201900043.

(22) Hasan, A. M. A.; Abdel-Raouf, M. E.-S. *Cellulose-Based Superabsorbent Hydrogels*; 2019. https://doi.org/10.1007/978-3-319-77830-3_11.

(23) Zhang, Y. S.; Khademhosseini, A. Advances in Engineering Hydrogels. *Science (80-.).* **2017**, *356* (6337). https://doi.org/10.1126/science.aaf3627.

(24) Anisha, S.; Kumar, S. P.; Kumar, G. V.; Garima, G. Hydrogels: A Review. *Artic. 016* **2010**, *4* (2).

(25) Kabiri, K.; Omidian, H.; Zohuriaan.Mehr, M. J.; Doroudiani, S. Superabsorbent Hydrogel Composites and Nanocomposites: A Review. *Polym. Polym. Compos.* **2010**, *16* (2), 101–113. https://doi.org/10.1002/pc.

(26) Chuin Tan, C. H.; Sabar, S.; Haafiz, M. K. M.; Garba, Z. N.; Hussin, M. H. The Improved Adsorbent Properties of Microcrystalline Cellulose from Oil Palm Fronds through Immobilization Technique. *Surfaces and Interfaces* **2020**, *20* (April). https://doi.org/10.1016/j.surfin.2020.100614.

(27) Zhang, T.; Wang, W.; Zhao, Y.; Bai, H.; Wen, T.; Kang, S.; Song, G.; Song, S.; Komarneni, S. Removal of Heavy Metals and Dyes by Clay-Based Adsorbents: From Natural Clays to 1D and 2D Nanocomposites. *Chem. Eng. J.* **2020**. https://doi.org/doi: https://doi.org/10.1016/j.cej.2020.127574.

(28) Dąbrowski, A. Adsorption - From Theory to Practice. *Adv. Colloid Interface Sci.* **2001**, *93* (1–3), 135–224. https://doi.org/10.1016/S0001-8686(00)00082-8.

(29) Rouquerol, F.; Rouquerol, J.; Sing, K. S. W.; Llewellyn, P.; Maurin, G. *Adsorption by Powders and Porous Solids Principles, Methodology and Applications*, Second edi.; Academic Press, 2014.

(30) Gerçel, O.; Gerçel, H. F. Adsorption of Lead (II) Ions from Aqueous Solutions by Activated Carbon Prepared from Biomass Plant Material of Euphorbia Rigida. *Chem. Eng. J.* **2007**, No. 132, 289–297.

(31) Mishra, P.; Patel, R. K. Removal of Lead and Zinc Ions from Water by Low Cost Adsorbents. *J. Hazard. Mater.* **2009**, No. 168, 319–325.

(32) Thompson, G.; Swain, J.; Kay, M.; Forster, C. . The Treatment of Pulp and Paper Mill Effluent: A Review, Bioresour. *Technol* **2001**, *1* (77), 275–286.

(33) Ruthven, D. M. *Principles of Adsorption and Adsorption Process*; John Wiley. & Sons: New York, 1984.

(34) Lowell, S. *Introduction to Powder Surface Area*; John Wiley. & Sons: New York, 1979.

(35) Gibbs, J. W. *Collected Works*, First edit.; Longmans: London, 1928.

(36) Brunauer, S., et al. No Title. *J. Am. Chem. Soc.* **1940**, No. 62, 1723.

(37) Jaroniec, M.; Madey, R. Physical Adsorption on Heterogeneous Solids. *Elsevier, Amsterdan* **1988**, *Chapter 1*.

(38) Sharma, S.; Tiwari, S. A Review on Biomacromolecular Hydrogel Classification and Its Applications. *Int. J. Biol. Macromol.* **2020**, *162*, 737–747. https://doi.org/10.1016/j.ijbiomac.2020.06.110.

(39) Ho, Y. S.; Mckay, G. Pseudo Second Order Model for Sorption Process. *Process Biochem* **1999**, No. 34, 451–465.

(40) Everett, D. H. IUPAC Manual Appendix II, Part I, Pure Appl. Chem. **1973**, *1* (31), 579.

(41) Rouquerol, J.; Avnir, D.; Faibridge, C. W. . et al. Pure Appl. Chem. **1994**, No. 66, 1793.

(42) Wang, J.; Guo, X. Adsorption Kinetic Models: Physical Meanings, Applications, and Solving Methods. *J. Hazard. Mater* **2020**, No. 390, 122–156.

(43) El-Khaiary, M. I.; Malash, G. F.; Ho, Y. S. On the Use of Linearized Pseudo-Second- Order

Kinetic Equations for Modeling Adsorption Systems. *Desaination* **2010**, *1* (257), 93–101.

(44) Plazinski, W.; Rudzinski, W.; Plazinska, A. Theoretical Models of Sorption Kinetics Including a Surface Reaction Mechanism: A Review. *Adv. Colloid Interface Sci.* **2009**, No. 152, 2–13.

(45) Crank, J. *Mathematics of Diffusion*; Oxford at the Clarendon Press: London, 1956.

(46) Boyd, G. E.; Adamson, A. W.; Meyes Jr, L. S. The Exchange Adsorption of Ions from Aqueous Solutions by Organite Zeolithes. II. Kinetics. *J. Am. Chem. Soc.* **1947**, No. 69, 2836.

(47) Morris, J. .; Weber, W. J. J. Adsorption of Biochemically Resistant Materials from Solution. In *Environmental Health Series AWTR-9. U.S. Department of Health, Education*; 1964.

(48) Pietrelli, L.; Francolini, I.; Piozzi, A.; Sighicelli, M.; Silvestro, I.; Vocciante, M. Chromium(III) Removal Fromwastewater by Chitosan Flakes. *Appl. Sci.* **2020**, *10* (6). https://doi.org/10.3390/app10061925.

(49) Geankoplis, C. J.; Leyva-Ramos, R. '"Model Simulation and Analysis of Surface Diffusion of Liquids in Porous Solids."' *Chem. Eng. Sci.* **1985**, *5* (40), 799.

(50) Lagergren, S. Zur Theorie Der Sogenannten Adsorption Geloster Stoffe Kungliga Svenska Vetenskapsakademiens. *Handlingar* **1898**, No. 24, 1–39.

(51) Ritchie, A. G. Alternative to the Elovich Equation for the Kinetics of Adsorption of Gases on Solids. *J. Am. Chem. Soc. Trans* **1977**, No. 73, 1650–1653.

(52) Langmuir, I. No Title. *J. Am. Chem. Soc.* **1917**, No. 39, 1848.

(53) Freundlinch, H. *Colloid and Capillary Chemistry*; Methuen and Co: London, 1926.

(54) Young, D. M.; Crowell, A. D. *Physical Adsorption of Gases*; Butterworths: London, 1962.

(55) Sips, R. J. *Chem. Phys.*; 1948.

(56) Snoeyink, V. L. et al. No Title. *Environ. Sci. Technol.* **1969**, No. 3, 918.

(57) Zogorski, J. S. *The Adsorption of Phenols onto Granular Activated Carbon from Aqueous Solutions*; Ph.D. dissertation, Rutgers University, Department of Environmental Science: New Brunswick, N.J., 1975.

(58) Gupta, V. K.; Ali, I. Environmental Water 1st Edition. In *Environmental Water (V. K. G. Ali)*; Elsevier: Amsterdan, 2013.

(59) Depeursinge, A.; Racoceanu, D.; Iavindrasana, J.; Cohen, G.; Platon, A.; Poletti, P.-A.; Muller, H. Desalination. *Remov. Ni(II) Zn(II) from an aqueous Solut. by reverse osmosis* **2010**, *174*, ARTMED1118. https://doi.org/10.1016/j.

(60) Riffat, R. *Fundamentals of Wastewater Treatment and Engineering*; CRC Press: Florida, USA, 2012.

(61) Baker, M. N. *The Quest for Pure Waster*, 2d ed.; American Water Works Association, Inc.: New York, 1981.

(62) Cheremisinoff, P. N. *Handbook of Water and Wastewater Treatment Technologies*; 2002; Vol. 60. https://doi.org/10.1016/s0167-8809(97)87011-9.

(63) Ramalho, R. S.; Beltrán, D. J.; de Lora, F. *Tratamiento de Aguas Residuales*; Reverte, Ed.: Quebec, 1996.

(64) Oviedo-Anchundia, R.; Moina-Quimí, E.; Naranjo-Morán, J.; Barcos-Arias, M. Contamination by Heavy Metals in the South of Ecuador Associated to the Mining Activity. *Bionatura* **2017**, *vol 1*. (2), 6. https://doi.org/10.21931/RB/2017.02.04.5.

(65) FUNSAD. Impactos en el ambiente y la salud por la minería del oro a pequeña escala en el Ecuador (segunda fase) http://www.funsad.org/Material/Material/INVESTIGACIO-NES/PuyangofaseII.pdf (accessed Sep 18, 2021).

(66) Denvir, D. M. J. V. T. "In Ecuador, mass mobilizations against mining confront President Correa" upsidedownworld.org/main/content/view/1588/49. (accessed Sep 19, 2021).

(67) Zapata, O. Industrial Wastewater Treatment and Reuse in a Developing Country Context :

Evidence at the Firm Level from Ecuador. **2018**, *4* (2). https://doi.org/10.1142/S2382624X17500059.

(68) Instituto Nacional de Estadística y Censo (INEC). Estadística de Información Ambiental Económica en Gobiernos Autónomos Descentralizados Municipales 2015 (Agua Y Alcantarillado) https://www.ecuadorencifras.gob.ec/documentos/web-inec/Encuestas_Ambientales/Municipios_2015/Documento_Tecnico-Gestion_de_Agua_y_Alcantarillado_2015.pdf (accessed Jun 2, 2021).

(69) Zapata, O. More Water Please, It's Getting Hot! The Effect of Climate on Residential Water Demand. *Water Econ. Policy* **2015**, No. 1, 3.

(70) SENAGUA. *Linea Base Para El Monitoreo de La Calidad Del Agua de Riego En La Demarcación Hidrográfica Del Guayas.*; Secretaría Nacional del Agua: Ecuador, 2010.

(71) Qadir, M.; Wichelns, D.; Raschid-Sally, L.; McCornick, P.; Dreschsel, P.; Bahri, A.; Minhas, P. The Challenges of Wastewater Irrigation in Developing Countries. Agricultural Water Management. **2010**, No. 97, 562–568.

(72) Lahive, E.; Jurkschat, K.; Shaw, B. J.; Handy, R. D.; Spurgeon, D. J.; Svendsen, C. Toxicity of Cerium Oxide Nanoparticles to the Earthworm Eisenia Fetida: Subtle Effects. *Environ. Chem.* **2014**, *11* (3), 268–278. https://doi.org/10.1071/EN14028.

(73) Justeau, C.; Victoria, A.; Gonzalez, V.; Jourdan, A.; Riess, J. G.; Krafft, M. P. Adsorption of Cerium Salts and Cerium Oxide Nanoparticles on Microbubbles Can Be Induced by a Fluorocarbon Gas Adsorption of Cerium Salts and Cerium Oxide Nanoparticles on Microbubbles Can Be Induced by a Fluorocarbon Gas. **2018**. https://doi.org/10.1021/acssuschemeng.8b01471.

(74) Hind, A. R.; Bhargava, S. K.; Mckinnon, A. At the Solid/Liquid Interface: FTIR/ATR-the Tool of Choice. *Adv. Colloid Interface Sci.* **2001**, No. 93, 91–114.

(75) McQuillan, A. J. Probing Solid-Solution Interfacial Chemistry with ATR-IR Spectroscopy of Particle Films. *Adv. Mater.* **2001**, No. 13, 1034–1038.

(76) Gulley-stahl, H.; Ii, P. A. H.; Schmidt, W. L.; Wall, S. J.; Buhrlage, A.; Bullen, H. A. Surface Complexation of Catechol to Metal Oxides: An ATR-FTIR, Adsorption, and Dissolution Study. *Environ. Sci. Technol* **2010**, *44* (11), 4116–4121.

(77) Eren, E.; Afsin, B. An Investigation of Cu(II) Adsorption by Raw and Acid-Activated Bentonite: A Combined Potentiometric, Thermodynamic, XRD, IR, DTA Study. *J. Hazard. Mater.* **2008**, *151* (2–3), 682–691. https://doi.org/10.1016/j.jhazmat.2007.06.040.

(78) Bubb, R. Chapter 7 : Basics of X-Ray Diffraction. *Scintag Inc.* **1999**, 1–25.

(79) Bozoğlan, B. K.; Duman, O.; Tunç, S. Preparation and Characterization of Thermosensitive Chitosan/Carboxymethylcellulose/Scleroglucan Nanocomposite Hydrogels. *Int. J. Biol. Macromol.* **2020**, *162*, 781–797. https://doi.org/10.1016/j.ijbiomac.2020.06.087.

(80) Nascente, P. A. P. Materials Characterization by X-Ray Photoelectron Spectroscopy. *J. Mol. Catal. A Chem* **2005**, No. 228, 145–150.

(81) Dambies, L.; Guimon, C.; Yiacoumi, S.; Guibal, E. Characterization of Metal Ion Interactions with Chitosan by X-Ray Photoelectron Spectroscopy. *Colloids Surf. A Physicochem. Eng. Asp.* **2001**, No. 177, 203–214.

(82) Vieira, R. S.; Oliveira, M. L. M.; Guibal, E.; Rodríguez-Castellón, E.; Beppu, M. M. Copper, Mercury and Chromium Adsorption on Natural and Crosslinked Chitosan Films: An XPS Investigation of Mechanism. *Colloids Surfaces A Physicochem. Eng. Asp.* **2011**, *374* (1–3), 108–114. https://doi.org/10.1016/j.colsurfa.2010.11.022.

(83) Sivaramaiah, S.; Reddy, P. R.; Reddy, V. K.; Reddy, T. S. Recent Developments of Derivative Spectrophotometry and Their Analytical Applications. *Chem. Eng. J.* **2004**, No. 49, 101. https://doi.org/https://doi.org/10.2116/analsci.21.595.

(84) Rozing, G. P. Deuterium L a m ~ Shutter Achromatlens Array Ell Grating. **1996**, *270*.

(85) Sánchez Rojas, F.; Bosch Ojeda, C. Recent Development in Derivative Ultraviolet/Visible Absorption Spectrophotometry: 2004-2008. A Review. *Anal. Chim. Acta* **2009**, *635* (1), 22–44. https://doi.org/10.1016/j.aca.2008.12.039.

(86) Mohammed, A.; Abdullah, A. Scanning Electron Microscopy (SEM): A Review. *Int. Conf. Hydraul. Pneum.* **2018**, *7* (January), 1–9.

(87) Nothnagle, P.; Chambers, W.; Davidson, M. Introduction to Stereomicroscopy https://www.microscopyu.com/techniques/stereomicroscopy/introduction-to-stereomicroscopy (accessed Oct 10, 2021).

(88) Rohindra, D. R.; Nand, A. V; Khurma, J. R. Swelling Properties of Chitosan Hydrogels 1 INTRODUCTION 3 RESULTS AND DISCUSSION. *South Pacific J. Nat. Appl. Sci.* **2004**, *22* (1), 32–35.

(89) Angumeenal, A. R.; Venkappayya, D. LWT - Food Science and Technology An Overview of Citric Acid Production. *LWT - Food Sci. Technol.* **2013**, *50* (2), 367–370. https://doi.org/10.1016/j.lwt.2012.05.016.

(90) Ciriminna, R.; Meneguzzo, F.; Delisi, R.; Pagliaro, M. Citric Acid: Emerging Applications of Key Biotechnology Industrial Product. *Chem. Cent. J.* **2017**, *11* (1), 1–9. https://doi.org/10.1186/s13065-017-0251-y.

(91) Seligra, P.; Medina Jaramillo, C.; Famá, L.; Goyanes, S. Biodegradable and Non-Retrogradable Eco-Films Based on Starch–Glycerol with Citric Acid as Crosslinking Agent. **2016**, No. 138, 66–74.

(92) Pagliaro, M.; Ciriminna, R.; Kimura, H.; Rossi, M.; Pina, C. Della. Minireviews Glycerol Chemistry From Glycerol to Value-Added Products. **2007**, No. May 2002, 4434–4440. https://doi.org/10.1002/anie.200604694.

(93) Tan, H. W.; Abdul Aziz, A. R.; Aroua, M. K. Glycerol Production and Its Applications as a Raw Material: A Review. *Renew. Sustain. Energy Rev.* **2013**, *27*, 118–127. https://doi.org/10.1016/j.rser.2013.06.035.

(94) M.N. Kumar; Muzzarelli, R. A.; Muzzarelli, C.; Sashiwa, H.; Domb, A. J. Chitosan Chemistry and Pharmaceutical Perspectives. *Chem. Rev. 104*. 2004, pp 6017–6084.

(95) Muzzarelli, R. A. A.; Muzzarelli, C. Chitosan Chemistry: Relevance to the Biomedical

Sciences, Polysaccharides 1: Structure, Characterization and Use. *Chem. Rev. 104*. 2005, pp 151–209.

(96) Dornish, M.; Kaplan, D.; Skaugrud, O. Standards and Guidelines for Biopolymers in Tissue-Engineered Medical Products: ASTM Alginate and Chitosan Standard Guides. *Am. Soc. Test. Mater. Ann.* **2001**, No. N. Y. Acad. Sci. 944, 388–397.

(97) Denkbas, E. B.; Ottenbrite, R. M. Perspectives on: Chitosan Drug Delivery Systems Based on Their Geometries. **2006**, No. J. Bioact. Compat. Polym. 21, 351–368.

(98) Riofrio, A.; Alcivar, T.; Baykara, H. The Environmental and Economic Viability of Chitosan Production in Guayas-Ecuador: A Robust Investment and Life Cycle Analysis. *ESPOL*.

(99) Ergun, R.; Guo, J.; Huebner-Keese, B. Cellulose. *Encycl. Food Heal.* **2015**, 694–702. https://doi.org/10.1016/B978-0-12-384947-2.00127-6.

(100) Javanbakht, S.; Shaabani, A. Encapsulation of Graphene Quantum Dot-Crosslinked Chitosan by Carboxymethylcellulose Hydrogel Beads as a PH-Responsive Bio-Nanocomposite for the Oral Delivery Agent. *Int. J. Biol. Macromol.* **2019**, *123*, 389–397. https://doi.org/10.1016/j.ijbiomac.2018.11.118.

(101) Kanikireddy, V.; Varaprasad, K.; Jayaramudu, T.; Karthikeyan, C.; Sadiku, R. Carboxymethyl Cellulose-Based Materials for Infection Control and Wound Healing: A Review. *Int. J. Biol. Macromol.* **2020**, *164*, 963–975. https://doi.org/10.1016/j.ijbiomac.2020.07.160.

(102) Calderón Salas, L. A. .; De Lima Eljuri, L.; Caetano Sousa, M. SYNTHESIS AND CHARACTERIZATION OF CHEMICALLY CROSS LINKED CARBOXYMETHYL CELLULOSE/CHITOSAN COMPOSITE HYDROGELS, 2021.

(103) Wojdyr, M. Fityk: A General-Purpose Peak Fitting Program. *J. Appl. Crystallogr.* **2010**, No. 43, 1126–1128.

(104) Ibitoye, E. B. et al. Extraction and Physicochemical Characterization of Chitin and Chitosan

Isolated from House Cricket. *Biomed. Mater.* **2018**, No. 13.

(105) Martín-López, H. et al. Structural and Physicochemical Characterization of Chitosan Obtained by UAE and Its Effect on the Growth Inhibition of Pythium Ultimum. *Agriculture* **2020**, *10*.

(106) Dharmalingam, K. Anandalakshmi, R. Fabrication, Characterization and Drug Loading Efficiency of Citric Acid Crosslinked NaCMC HPMC Hydrogel Films for Wound Healing Drug Delivery Applications. *Int. J. Biol. Macromol* **2019**, No. 134, 815–829.

(107) Priyadarshi, R.; Sauraj, Kumar, B.; Negi, Y. S. Chitosan Film Incorporated with Citric Acid and Glycerol as an Active Packaging Material for Extension of Green Chilli Shelf Life. *Carbohydr. Polym.* **2018**, No. 195, 329–338.

(108) Wu, H. et al. Effect of Citric Acid Induced Crosslinking on the Structure and Properties of Potato Starch/Chitosan Composite Films. *Food Hydrocoll.* **2019**, No. 97, 105–208.

(109) Cai, B. et al. Preparation, Characterization and in Vitro Release Study of Drug-Loaded Sodium Carboxy Methylcellulose/Chitosan Composite Sponge. *PLoS One* **2018**, No. 13, 206–275.

(110) Zhi, X.; Du, B.; Yuan, S. Preparation of Elastic and Antibacterial Chitosan–Citric Membranes with High Oxygen Barrier Ability by in Situ Cross-Linking. *ACS Omega* **2020**, No. XXXX.

(111) Kong, Q.; Wang, X.; Lou, T. Preparation of Millimeter-Sized Chitosan Carboxymethyl Cellulose Hollow Capsule and Its Dye Adsorption Properties. *Carbohydr. Polym.* **2020**, No. 244, 116–481.

(112) Machado, B. R. et al. Bactericidal Pectin/Chitosan/Glycerol Films for Food Pack Coatings: A Critical Viewpoint. *Int. J. Mol. Sci* **2020**, No. 21, 8663.

(113) Capanema, N. et al. Eco-Friendly and Biocompatible Crosslinked Carboxymethylcellulose Hydrogels as Adsorbents for the Removal of Organic Dye Pollutants for Environmental Applications. *Environ. Technol.* **2017**, No. 39, 1–42.

(114) Largitte, L.; Pasquier, R. A Review of the Kinetics Adsorption Models and Their Application to the Adsorption of Lead by an Activated Carbon. *Chem. Eng. Res. Des.* **2016**, *109*, 495–504. https://doi.org/10.1016/j.cherd.2016.02.006.

APPENDIX A:

Table 15. kinetic model adsorption.

Models	Differential equation	Nonlinear form	Linear form	Linear plot
Fick equation		-	-	-
Crank		$\frac{Q}{Q_{max}} = 1 - \frac{6}{\pi^2}\sum_{n=1}^{\infty}\frac{1}{n^2}\exp\left(\frac{-D_s n^2 \pi^2 t}{R^2}\right)$	-	-
Crank (short times) $Q/Q_{max} < 0.3$		$\frac{Q}{Q_{max}} = 6\left(\frac{D_s t}{R^2}\right)^{1/2}\left[\pi^{\frac{1}{2}} - \frac{1}{2}\left(\frac{D_s t}{R^2}\right)^{\frac{1}{2}}\right]$	$Ln\left(\frac{Q}{Q_{max}}\right) = \frac{1}{2}Lnt + Ln\left[\pi^{\frac{1}{2}} - \frac{1}{2}\left(\frac{D_s t}{R^2}\right)^{\frac{1}{2}}\right] + \frac{1}{2}Ln\left(\frac{D_s}{R^2}\right) + Ln6$	-
Simplification Crank Short times		$Q = kt^{1/2}$ with $k = 6\left(\frac{D_s}{\pi R^2}\right)^{1/2}$	$Ln\,Q = \frac{1}{2}Ln(t) + Ln(k)$	$Ln\,Q = f(Lnt)$

Weber and Morris		$Q = kt^{1/2} + Cte$; $q_t = k_{W\&M}t^{1/2}$	-	-
Bangham		$Q = kt^{\vartheta}$	$Ln\ Q = \vartheta Ln(t) + Ln\ (k)$	$Ln\ Q = f(Lnt)$
Boyd, Crank long times: $Q/Q_{max} > 0.85$	$\frac{dq_t}{dt} = R(q_\infty - q_t)$	$\frac{Q}{Q_{max}} = 1 - \frac{6}{\pi^2}\exp\left(\frac{-D_s\pi^2 t}{R^2}\right)$; $q_t = q_\infty(1 - e^{Rt})$	$Ln\left(1 - \frac{Q}{Q_{max}}\right) = Ln\left(\frac{6}{\pi^2}\right) - \frac{-D_s\pi^2 t}{R^2}$	$Ln\ (1 - cteQ) = f(t)$
Geankoplis and Leyva-Ramos		$V\frac{dC}{dt} = -msk_L(C - C_r\|_{r=R})$ $\varepsilon\frac{\partial C_r}{\partial t} + \rho_P\frac{\partial Q}{\partial t}) = \frac{1}{r^2}\frac{\partial}{\partial r}\left[r^2\left(D_{ep}\frac{\partial C_r}{\partial r} + D_s\rho_P\frac{\partial Q}{\partial r}\right)\right]\frac{\partial C_r}{\partial t}\|_{r=0}$ $D_{ep}\frac{\partial C_r}{\partial r} + D_s\rho_P\frac{\partial Q}{\partial r} = k_L(C - C_r\|_{r=R})$ $t = 0\ ; C = C_0$	-	-

		$t = 0;\ C_r = 0; 0 \leq r\ \leq R$ $Q(r) = f(C_r)$		
Langmuir (1 site)	$\frac{dq_t}{dt} = k_a\left(C_0 - \frac{mq_t}{V}\right)(q_{max} - q_t) - \frac{k_a}{K_L}q_t$	$Q = Q_{max}\left(\frac{k'_{ad}}{k'_{ad} + k_d}\right)(1 - e^{-(k'_{ad}+k_d)t})$	$Ln\left\{1 - \frac{Q}{Q_{max}\left(\frac{k'_{ad}}{k'_{ad}+k_d}\right)}\right\} = -(k'_{ad} + k_d)t$	$Ln(1 - cteQ) = f(t)$
Pseudo first order PFO	$\frac{dq_t}{dt} = k_1(q_e - q_t)$	$Q = Q_{max}(1 - e^{-k'_{ad}t});$ $q_t = q_e(1 - e^{k_1 t})$	$Ln\left(1 - \frac{Q}{Q_{max}}\right) = -k'_{ad}t$	
Pseudo second order PSO	$\frac{dq_t}{dt} = k_2(q_e - q_t)^2$	$Q = \frac{(k'_{ad}Q^2{}_{max})t}{1+k'_{ad}Q_{max}t};$ $q_t = \frac{q_e{}^2 k_2 t}{1 + q_e k_2 t}$	$\frac{t}{Q} = \frac{t}{Q_{max}} + \frac{1}{k'_{ad}Q^2{}_{max}}$	$t/Q_t = f(t)$

Pseudo order n For n ≠ 0	$\frac{dq_t}{dt} = k_1(q_e - q_t) + k_2(q_e - q_t)^2$	$Q = Q_{max}\left\{1 - \left[\frac{Q}{1 + k'_{ad}(n-1)Q^{n-1}_{max}t}\right]^{\frac{1}{n-1}}\right\}$	-	-
Elovich	$\frac{dq_t}{dt} = ae^{bq_t}$	$Q = \frac{1}{\beta}Ln(1 + \alpha\beta t)$; $q_t = \frac{1}{b}\log(1 + abt)$	$LnQ = Ln\left(\frac{1}{\beta}\right) + Ln^2(1 + \alpha\beta t)$	-
Simplification of Elovich: 1<< $\alpha\beta t$		$Q = \frac{1}{\beta}Ln(\alpha\beta t)$	$Q = \frac{1}{\beta}Ln(\alpha\beta) + \frac{1}{\beta}lnt$	$Q = f(Lnt)$

Taken from Largitte and Pasquier[114].

a	Initial adsorption rate constant of the Elovich model (mg g^{-1})
A	Constant of the Boyd's equationM
b	Desorption rate constant of the Elovich model (g mg^{-1})
B	Boyd's coefficient (minh−1)
C_0	Initial adsorbate concentration (mg·L^{-1})
C_e	Equilibrium adsorbate concentration (mg·L^{-1})
C_t	Adsorbate concentration at time t (mg·L^{-1})
k_1	Pseudo-first-order rate constant (min^{-1})
K_2	Pseudo-second-order rate constant (min^{-1})
K_a	Adsorption rate constant (L·mg^{-1}·min^{-1})
$k_{F\&S}$	Mass transfer coefficient between the bulk liquid and the surface surface of the adsorbent (cm·min^{-1})
K_L	Langmuir constant (L·mg^{-1})
$K_{W\&M}$	Intraparticle diffusion coefficient (mg·g·$min^{-1/2}$)
m_s	Mass of adsorbent per unit volume of solution (g·L^{-1})
q_∞	Equilibrium adsorption capacity at infinite time (mg·g^{-1})
q_{cal}	Calculated adsorption capacity (mg·L−1)
q_e	Adsorption capacity at equilibrium (mg·L−1)
q_{et}	Equilibrium adsorption capacity in the pores of the adsorbent (mg·g^{-1})
q_{exp}	Experimental adsorption capacity (mg·L^{-1})

q_m	Maximum adsorption capacity ($mg \cdot g^{-1}$)
q_{max}	Langmuir constant ($mg \cdot g^{-1}$)
q_t	Adsorbed amount of the adsorbate at time t ($mg \cdot L^{-1}$)
t	Adsorption time (min)
V	Solution volume (L)